

1 **Environmental forcing does not induce diel or synoptic**
2 **variation in carbon isotope content of forest soil**
3 **respiration**

4

5 **David R. Bowling^{1*}, Jocelyn E. Egan², Steven J. Hall³, David A. Risk⁴**

6 [1]{Dept. of Biology, Univ. of Utah, Salt Lake City, Utah, USA}

7 [2]{Dept. of Earth Sciences, Dalhousie University, Halifax, Nova Scotia, Canada}

8 [3]{Global Change and Sustainability Center, Univ. of Utah, Salt Lake City, Utah, USA}

9 [4]{Dept. of Earth Sciences, St. Francis Xavier University, Antigonish, Nova Scotia, Canada}

10 Correspondence to: D. R. Bowling (david.bowling@utah.edu)

11

12

13

14

15

1 **Abstract**

2 Recent studies have examined temporal fluctuations in the amount and carbon isotope content
3 ($\delta^{13}\text{C}$) of CO_2 produced by respiration of roots and soil organisms. These changes have been
4 correlated with diel cycles of environmental forcing (e.g., sunlight and soil temperature) and
5 with synoptic-scale atmospheric motion (e.g., rain events and pressure-induced ventilation).
6 We used an extensive suite of measurements to examine soil respiration over two months in a
7 subalpine forest in Colorado, USA (the Niwot Ridge AmeriFlux forest). Observations
8 included automated measurements of CO_2 and $\delta^{13}\text{C}$ of CO_2 in the soil efflux, the soil gas
9 profile, and forest air. There was strong diel variability in soil efflux, but no diel change in
10 the $\delta^{13}\text{C}$ of the soil efflux (δ_{R}) or the CO_2 produced by biological activity in the soil (δ_{J}).
11 Following rain, soil efflux increased significantly, but δ_{R} and δ_{J} did not change. Temporal
12 variation in the $\delta^{13}\text{C}$ of the soil efflux was unrelated to measured environmental variables, and
13 we failed to find an explanation for this unexpected result. Measurements of the $\delta^{13}\text{C}$ of the
14 soil efflux with chambers agreed closely with independent observations of the isotopic
15 composition of soil CO_2 production derived from soil gas well measurements. Deeper in the
16 soil profile and at the soil surface, results confirmed established theory regarding diffusive
17 soil gas transport and isotopic fractionation. Deviation from best-fit diffusion model results at
18 the shallower depths illuminated a pump-induced ventilation artifact that should be
19 anticipated and avoided in future studies. There was no evidence of natural pressure-induced
20 ventilation of the deep soil. However, higher variability of $\delta^{13}\text{C}$ of the soil efflux relative to
21 $\delta^{13}\text{C}$ of production derived from soil profile measurements was likely caused by transient
22 pressure-induced transport with small horizontal length scales.

23

24

1 **1 Introduction**

2 The efflux of CO₂ from soils results from the collective contribution of a host of organisms
3 with diverse physiology. Processes influencing soil respiration are complex and vary based
4 on a variety of biological, biophysical, and biogeochemical factors. World soils are a major
5 storage reservoir for carbon, and soil respiration represents the largest gross transfer of carbon
6 to the atmosphere, much larger than anthropogenic sources (Le Quéré et al., 2013; Raich and
7 Schlesinger, 1992). Understanding the complicated role of the biosphere in the global carbon
8 cycle is thus essential for prediction of future climate (Friedlingstein et al., 2014; Heimann
9 and Reichstein, 2008).

10 Respiration by soils is dependent on temperature and moisture (Davidson et al., 1998; Lloyd
11 and Taylor, 1994), the composition of the community of soil organisms (Bardgett et al.,
12 2008), and the quality of organic compounds used to fuel heterotrophic metabolism (Conant
13 et al., 2011). In addition, there is strong evidence that soil respiration is linked to plant
14 photosynthesis (Kuzyakov and Gavrichkova, 2010). Because of this linkage, a large fraction
15 of carbon in the soil efflux has resided in the biosphere for only hours to days to weeks
16 (Högberg et al., 2001).

17 The connection between photosynthesis and soil respiration has led many to examine the
18 stable carbon isotopic composition ($\delta^{13}\text{C}$) of respiration in the context of environmental
19 controls on photosynthesis such as sunlight, soil moisture, and humidity (Bowling et al.,
20 2008). For example, changes in soil moisture and humidity influence stomatal conductance
21 of C3 plants, altering photosynthetic discrimination, leading via root respiration or exudation
22 to changes in $\delta^{13}\text{C}$ of soil efflux and whole forest respiration (Ekblad and Högberg, 2001; Lai
23 et al., 2005). Others have used $\delta^{13}\text{C}$ of soil efflux to assess the relative contributions of
24 autotrophic and heterotrophic respiration (Kuzyakov, 2006), or added isotopic labels via
25 organic material (Bird and Torn, 2006) or via photosynthesis (Hogberg et al., 2008) to
26 investigate soil carbon cycle processes. Several studies have identified diel variation in the
27 $\delta^{13}\text{C}$ of plant and soil respiration (reviewed by Werner and Gessler, 2011), and others have
28 highlighted changes in rate and $\delta^{13}\text{C}$ of soil efflux following rain (e.g., Jarvis et al., 2007;
29 Unger et al., 2012). Presumably such changes involve varied consumption of organic
30 substrates for heterotrophic activity that differ systematically in $\delta^{13}\text{C}$, such as starch, lignin, or
31 cellulose (Bowling et al., 2008). However, there are a wide variety of post-photosynthetic

1 fractionation processes that influence the $\delta^{13}\text{C}$ of respiration and of CO_2 in the soil, many of
2 which are poorly understood (Brüggemann et al., 2011; Ghashghaie and Badeck, 2014).

3 Many ecologists use soil efflux as a measure of the simultaneous rate of production within the
4 soil. (In this paper we use “soil efflux” to refer to the rate of transport of CO_2 from the soil
5 surface to the atmosphere, “soil CO_2 ” to refer to the mole fraction of CO_2 in the soil pore
6 space with respect to dry air, and “production” to refer to the process rate of biological
7 production of CO_2 by soil organisms and roots). However, soil efflux and production are not
8 always tightly coupled. Permeable soils are subject to ventilation by wind or pressure
9 changes (e.g., Flechard et al., 2007), with sometimes dramatic changes in soil CO_2 over just a
10 few hours or days (Sánchez-Cañete et al., 2013). Sometimes ventilation is less obvious, but
11 comparison of measurements of soil efflux and soil CO_2 with models of diffusive transport
12 suggests that ventilation may be persistent in some soils (Roland et al., 2015). Because
13 aerobic respiration involves CO_2 production that is stoichiometrically related to O_2
14 consumption, the ratio of these two fluxes (apparent respiratory quotient or ARQ) can be used
15 to identify the presence of other processes in the soil that can lead to decoupling between CO_2
16 efflux and production. The ARQ method has highlighted the importance of CO_2 dissolution
17 in soil water, carbonate dissolution and precipitation, and possibly oxidation of reduced iron
18 (Angert et al., 2015). Finally, CO_2 transported through the xylem can be similar in magnitude
19 to soil efflux (Aubrey and Teskey, 2009). All of these factors would lead to differences in the
20 rates of production within the soil and soil efflux.

21 Due to fractionation associated with diffusion, stable isotopes of CO_2 provide a useful means
22 to examine soil gas transport processes. There is a well-established physical understanding of
23 the transport of CO_2 and its stable isotope variants within soils (Amundson et al., 1998;
24 Cerling, 1984; Cerling et al., 1991). Carbon dioxide within the soil pore space reflects the
25 dynamic mixing of biological production (which varies in time and space) with atmospheric
26 CO_2 under the influence of diffusion. Modeled diffusive profiles of soil CO_2 (which we
27 denote C_s) and $\delta^{13}\text{C}$ of CO_2 in the soil (δ_s) are shown in Fig. 1. (See Table 1 for a complete
28 list of symbols; model details are provided in section 2.7). The presence of air at the soil
29 surface forces a boundary condition so that C_s and δ_s must match the CO_2 and isotope ratio of
30 forest air (C_a and δ_a , circles). Within the soil, CO_2 increases with depth, with higher CO_2 in
31 the soil pore space under conditions of higher biological production (Fig. 1a; the colored lines
32 differ only in the rates of production). There is a corresponding decrease in δ_s with depth,

1 more negative with higher production (Fig. 1b). The isotopic composition of production in
2 these simulations was fixed at -26 ‰ in both high and low production scenarios (squares in
3 Fig. 1b,c).

4 Due to the difference in mass of $^{12}\text{CO}_2$ and $^{13}\text{CO}_2$, transport by molecular diffusion of CO_2 in
5 air leads to a 4.4 ‰ fractionation (Cerling et al., 1991). Hence δ_s in the bulk gas within the
6 soil profile is never equal to the signature of production (-26 ‰), instead it is always enriched
7 (less negative, compare dashed line to colored lines in Fig. 1b). Note, however, that due to
8 mixing with atmospheric CO_2 , the difference between the signature of production (dashed
9 line) and δ_s can be much greater than 4.4 ‰, especially near the surface and when the rate of
10 production is low.

11 The mixing of CO_2 from biological production (square) with forest air (circle) is illustrated in
12 Fig. 1c. If there were no diffusion, mixing of these two sources would follow a linear
13 combination reflecting the proportion of each (dashed line, Keeling, 1958). Instead, mixing
14 by diffusion follows the upper line, and the $\delta^{13}\text{C}$ vs. $1/\text{CO}_2$ relation is identical in both the
15 high and low production cases. The y-intercepts of the upper and lower lines differ by 4.4 ‰.
16 Under fully diffusive conditions, the isotopic composition of biological production (square,
17 δ_j) can be calculated from a pair of measurements of CO_2 in air (circle, C_a , δ_a) and in the soil
18 pore space (triangle, C_s , δ_s) using this equation (derived by Davidson, 1995):

$$19 \quad \delta_j = \frac{C_s(\delta_s - 4.4) - C_a(\delta_a - 4.4)}{1.0044(C_s - C_a)} \quad (1)$$

20 Mixing of soil-respired CO_2 with air under conditions that involve even a minor amount of
21 advection, such as with windy conditions within a snowpack, will lead to C_s and δ_s that fall
22 between the two lines in Fig. 1c (Bowling et al., 2009; Bowling and Massman, 2011). We
23 anticipate that this pattern would be observed in any porous medium (such as a soil) where
24 diffusion dominates transport that is exposed to ventilation by pressure or wind forcing, even
25 if very low bulk fluid flow is involved. Further, the vertical profiles of C_s and δ_s in soils
26 during ventilation should deviate from fully diffusive profiles like those in Fig. 1a, b.

27 Given the complexities of the many biological and physical processes influencing the isotopic
28 content of CO_2 in soil-atmosphere exchange, and the wide variety of ways that isotopes of
29 CO_2 have been used to interpret those processes, we were motivated to conduct an extensive
30 observational study. We used three independent measurement methods combined with soil

1 gas transport modeling to continuously examine CO₂ in the soil pore space, forest air, and soil
2 efflux in a high-elevation subalpine forest to test the following hypotheses:

- 3 1) The $\delta^{13}\text{C}$ of soil efflux changes on a daily (diel) basis.
- 4 2) Rain following a dry period leads to changes in $\delta^{13}\text{C}$ of soil efflux as the activity of
5 the soil heterotrophic community is altered.
- 6 3) Barometric pressure changes associated with passage of weather systems leads to
7 ventilation of the soil gas profile.

8

9 **2 Methods**

10 **2.1 Study Location**

11 This study was conducted at the Niwot Ridge AmeriFlux forest (<http://ameriflux.lbl.gov>) in
12 the Rocky Mountains of Colorado, United States (40.03° N, 105.55° W, 3050 m elevation).
13 The subalpine forest is dominated by the conifer species *Pinus contorta*, *Picea engelmannii*,
14 and *Abies lasiocarpa*, with sparse understory cover of *Vaccinium* species, lichens, and
15 mosses. The forest is on a late-Pleistocene glacial moraine with generally thin (mean 60 cm)
16 sandy/rocky Inceptisols covered by a thin (< 10 cm) organic horizon (Cole and Braddock,
17 2009; Lewis and Grant, 1979; Scott-Denton et al., 2003; Xiong et al., 2011). The site includes
18 a highly-instrumented tower from which biosphere-atmosphere exchange of CO₂ has been
19 monitored since 1998 (Monson et al., 2002). Barometric pressure and wind data were
20 obtained from the AmeriFlux data archive (<http://ameriflux.lbl.gov/>) for this study.

21 **2.2 Experimental Design**

22 Field observations were conducted during August-September 2011 (65 days total) in an
23 undisturbed area within 30 m of the flux tower (see image in Fig. 2). Three soil locations
24 were selected at random within 5 m of a short mast where continuous measurements of forest
25 air CO₂ and its isotopes have been made for over 9 years (Bowling et al., 2014). At each
26 location, an automated soil chamber was installed to monitor soil efflux, and adjacent to each
27 chamber, soil temperature (107 thermistor probe, Campbell Scientific, Inc., Logan, Utah,
28 USA) was measured at the interface of the organic and mineral horizons (O/A interface). Soil
29 moisture was monitored in the O horizon and the top 10 cm of the A horizon with a single

1 depth-integrating sensor (CS615 water content reflectometer, Campbell Scientific, Inc.,
2 Logan, Utah, USA). Gas wells were installed at four depths surrounding each chamber to
3 monitor soil pore gas. The chambers and gas wells were connected to a central analyser to
4 measure soil gas composition (see next sections).

5 **2.3 CO₂ and its isotopes**

6 Carbon dioxide mole fraction and carbon isotope ratio in chamber, soil pore space, and forest
7 air were measured using tunable diode laser absorption spectroscopy (TDLAS, TGA100A,
8 Campbell Scientific, Inc., Logan, UT, USA). The TDLAS instrument and calibration
9 procedure has been described elsewhere (Bowling et al., 2009; Schaeffer et al., 2008).
10 Observations are presented relative to the World Meteorological Organization CO₂ Mole
11 Fraction Scale (WMO X2007) and the International Atomic Energy Agency Vienna Pee Dee
12 Belemnite (VPDB) scale, respectively. High CO₂ mole fractions in the soil were diluted with
13 CO₂-free air using mass flow controllers into the measurable range for the analyser (Bowling
14 et al., 2009). Measured flow rates were used to calculate mole fractions of the original soil
15 gas, which usually exceeded the defined range of the WMO X2007 scale (maximally 521
16 $\mu\text{mol mol}^{-1}$).

17 **2.4 Automated soil chambers and δ_R**

18 Small (< 1 Pa) chamber-air pressure gradients have been shown to erroneously and markedly
19 influence soil CO₂ efflux (Fang and Moncrieff, 1998). Given the diffusive fractionation for
20 CO₂ isotopes, for our application it was critical to use chambers that would minimally disturb
21 the soil diffusive environment. Steady state dynamic chambers were used following the
22 design of Rayment and Jarvis (1997) to minimize differential pressure between the chamber
23 and the soil (Fig. 2). Laboratory tests with the chambers sealed to a solid impermeable bench
24 top (Xu et al., 2006) indicated that chamber-air differential pressure was less than 0.2 Pa at
25 flow rates below and including 4 L min⁻¹ (data not shown), so 4 L min⁻¹ was used in the field.
26 Closure of chambers was automated using pneumatic pistons following the design of Riggs et
27 al. (2009).

28 One chamber was measured each hour, with each chamber measured on staggered 3-h
29 intervals (8 measurements per chamber per day). During a measurement, chamber lids were
30 closed for 20 minutes. CO₂ in the inlet and outlet were monitored for alternating one-minute

1 periods while the chamber was closed using an infrared gas analyser (LI-820, LI-COR,
2 Lincoln, NE, USA). During closure, CO₂ in the outlet increased slowly and then stabilized as
3 a new steady state was reached. TDLAS measurements were made during the last 6 minutes
4 of the closure period, continuing to alternate measurement of the inlet and outlet of the
5 chamber for 1 minute each (but always with constant flow through the chamber). The CO₂
6 mole fraction difference between inlet and outlet during the last 6 minutes was stable and
7 averaged $81 \pm 21 \mu\text{mol mol}^{-1}$ (mean and standard deviation, n=1284 chamber measurements).
8 The soil CO₂ efflux and $\delta^{13}\text{C}$ of soil efflux (which we will refer to as δ_{R}) were calculated from
9 the CO₂ and $\delta^{13}\text{C}$ measurements of the inlet and outlet gas streams using equations provided
10 by Moyes et al. (2010).

11 **2.5 Gas wells and δ_{J}**

12 Gas wells were used to monitor soil pore gas with as little disturbance as possible – no
13 digging was required except for the shallowest that required minor digging. Wells were
14 installed at four depths within 1m horizontally of each chamber (12 total wells); these were at
15 the O/A interface and 5, 10, and 30 cm below the top of the mineral soil. The O/A interface
16 wells were 10 cm diam. x 1 cm tall stainless steel cylinders with steel mesh on the top and
17 bottom (Sommerfeld et al., 1991), inserted by hand. Remaining wells were made of 6 mm
18 OD stainless steel tubing, inserted vertically into the soil surface with a hammer. A metal rod
19 was used during insertion to prevent clogging the tube with soil or roots, and then the rod was
20 removed. All gas wells were attached to a 1.0 μm PTFE filter (Acro-50, Pall Corporation,
21 East Hills, NY, USA) and connected to the TDLAS sampling manifold with variable lengths
22 (tens of m) of 6 mm OD tubing (Type 1300, Synflex Specialty Products, Mantua, OH, USA).
23 The volume of each length of tubing was measured after field installation using a pressure
24 change when adding evacuated tubing to a known volume using the ideal gas law. This
25 allowed soil gas to be pumped to the analyser at a controlled flow rate with a known arrival
26 time. This was tested repeatedly in the field by introducing a step change in CO₂ in each
27 length of tubing and watching for its arrival at the analyser. Sampling flow rate was 235 mL
28 min^{-1} , and gas flowed in each inlet for 10 min during measurement. The 10-sec period
29 immediately following arrival of the gas at the end of the tubing was averaged for each
30 measurement. Thus the perturbation to the soil gas well involved a total volume of 2.35 L,
31 and 3 h elapsed before the next measurement of a given well. The 4 gas wells surrounding a

1 chamber were measured in a 20-min period, and this was repeated every three hours
2 (offsetting the 3 chamber locations each hour), providing 8 measurements per day for each
3 well. The wells surrounding each chamber were measured 3 h after the chamber was
4 measured to avoid disrupting each type of observation with the other. In total there were
5 4350 gas well measurements made (69% coverage due to occasional clogging with water or
6 power loss).

7 The isotopic composition of belowground CO₂ production (δ_j) was calculated for all
8 individual gas well measurement pairs (C_s , δ_s) using Eq. 1. The forest air inlet to the soil
9 surface chamber nearest the well was used for C_a and δ_a , interpolated to match the gas well
10 measurement in time using a piecewise Hermite interpolation (Matlab R2013a, The
11 Mathworks, Natick, MA, USA).

12 **2.6 Carbon isotope content of whole-forest respiration (δ_F)**

13 The $\delta^{13}\text{C}$ of whole-forest respiration (δ_F) was calculated for the entire study period from
14 mixing lines (Ballantyne et al., 2011) between CO₂ and $\delta^{13}\text{C}$ of CO₂ in forest air at 9 heights,
15 using nighttime data only. This involved removal of synoptic changes in the composition of
16 air by subtracting the observation at the top of the tower; details can be found in Bowling et
17 al. (2014).

18 **2.7 Soil diffusive gas transport model**

19 To test the hypothesis that barometric pressure change to ventilation of the soil pore space, we
20 compared soil pore space observations (C_s , δ_s) to model simulations produced using a steady-
21 state soil gas transport model (Cerling, 1984; Nickerson et al., 2014). The model was based
22 on Fick's second law of diffusion:

$$23 \quad \theta \frac{\partial X}{\partial t} = \frac{\partial}{\partial z} \left(D(z, t) \frac{\partial X}{\partial z} \right) + P(z, t) \quad (2)$$

24 where θ is the air-filled porosity of the soil, X is the gas concentration, $D(z, t)$ is the soil gas
25 diffusivity and $P(z, t)$ represents biological production as a function of depth (z) and time (t).
26 We assumed steady-state conditions ($dX/dt = 0$), soil gas diffusivity was constant with depth
27 ($D(z)=D$), and biological production decreased exponentially with depth as

$$28 \quad P(z) = \frac{P_0}{\lambda} e^{-z/\eta} \quad (3)$$

1 where P_0 is the total soil efflux (production integrated over the entire soil depth), η is the
2 depth at which production is reduced to $1/e$ of its value at $z=0$ (e -folding depth), and λ is a
3 parameter which constrains production to occur within the soil depths 0 to L , where L is the
4 lower (z) model boundary, with no CO_2 production or diffusion occurring below it. The upper
5 soil surface must interact with the air in the forest providing an upper model boundary
6 condition,

$$7 \quad X(z=0) = \rho_a C_a \quad (4)$$

8 and assumption of a no-flux lower boundary provided a second

$$9 \quad \left. \frac{\partial X}{\partial z} \right|_{z=L} = 0 \quad (5)$$

10 Similar steady-state equations were used for $^{12}\text{CO}_2$ and $^{13}\text{CO}_2$ treating each isotopologue of
11 CO_2 as an independent gas with its own diffusivity and biological production rate (Cerling et
12 al., 1991). For full derivation of both steady-state equations see Nickerson et al. (2014).

13 The above equations were solved numerically (Mathematica NDSolve version 9.0.1; Wolfram
14 Research, Champaign, IL, USA) using a broad range of values for each parameter, with
15 coarse steps. Model best fits were determined (see below) and model parameter optimization
16 was performed, where the optimized model produced ~ 600 synthetic solutions with the
17 following parameters: soil gas diffusivity (D ; $5e^{-6}$ to $8e^{-6}$ m^2/sec in steps of 0.5), e -folding
18 depth (η ; 0.01 to 0.60 m in steps of 0.1), and model lower boundary depth (L ; 0.3 to 2 m in
19 steps of 0.1). Mean values for the rate of production (P_0), $\delta^{13}\text{C}$ of production, CO_2 mole
20 fraction and $\delta^{13}\text{C}$ of CO_2 in forest air were determined from measurements (soil efflux, δ_R , C_a ,
21 δ_a , respectively) for time periods of interest (described in Results) and used as forcing input.

22 Model results consisted of a family of gas profiles for the range of parameters examined, and
23 were entirely independent of the soil pore space observations. Model output consisted of
24 $^{12}\text{CO}_2$ and $^{13}\text{CO}_2$ concentration profiles (in 1 cm increments) that were converted to CO_2 and
25 $\delta^{13}\text{C}$ profiles. These were compared to measured gas profiles in the soil (mean values for C_S
26 and δ_S over the period of interest), by calculating the root mean square (RMS) difference
27 between the model output and the measured values at the depths of measurement. A best-fit
28 diffusion model result was selected by optimizing for both CO_2 and $\delta^{13}\text{C}$ by minimizing the
29 dimensionless error metric

1
$$\varepsilon = \left(\frac{RMS(C_S)}{range(C_S)} \right) \left(\frac{RMS(\delta_S)}{range(\delta_S)} \right) \quad (6)$$

2 where each individual root-mean-square (RMS) error (for C_S or δ_S) was normalized by the
3 range of values observed for that time period.

4 The model-data comparison was conducted 1) using observations from all gas well
5 measurement depths, and 2) using only the lowest 3 depths (omitting measurements from the
6 O/A interface). The latter was done after identifying a measurement artifact that will be
7 described below.

8

9 **3 Results**

10 Time series of soil moisture and temperature are shown with efflux data from chamber 1 in
11 Fig. 3 (data from the other chambers were similar). Soil temperature varied by as much as 10
12 °C on a diel basis and led to significant diel variability in soil efflux (Table 2, Fig. 3). Soil
13 efflux was systematically higher in chamber 3 compared to the others, although soil
14 temperature was similar (Table 2). There were several rain events during the study; five-day
15 periods with dry soil and after the first large rain event were selected for closer analysis
16 (“dry” and “moist” periods, shaded in Fig. 3). The first major rain event increased soil efflux
17 by 26-39 % during the moist period relative to the dry period, but there was no concurrent
18 change in soil temperature (Table 2, Fig. 3). The $\delta^{13}C$ of soil efflux was quite variable,
19 especially during the first half of the record, but neither the variability nor the mean changed
20 in response to rain during the dry-moist period comparison (Table 2, Fig. 3). Later in the
21 record after several rain events the variability decreased.

22 Rainfall did lead to systematic and sustained changes in belowground CO_2 and its isotopic
23 content (Fig. 4), but these changed together and thus δ_j was not affected. The CO_2 in the soil
24 increased markedly following wetting, especially at depth. Pressure and wind speed varied
25 with synoptic-scale atmospheric motion (Fig. 4). These quantities were only weakly related
26 to changes in C_S and δ_S , which appeared to respond to wetting and its influence on diffusion
27 and production rather than to ventilation. These data (C_S , δ_S) were combined with
28 measurements of forest air (C_a , δ_a , Fig. 4) to calculate time series of δ_j at each depth (shown
29 later) using Eq. 1.

1 There was strong diel variability in soil temperature (coefficient of variation $CV = 8-11\%$,
2 Table 2) and soil efflux ($CV = 7-13\%$), but no diel variability in the isotopic content of soil
3 efflux ($CV < 2\%$, Fig. 5, Fig. S1). Normalized diel patterns were nearly identical during the
4 dry and moist periods for all chambers (Fig. 5), despite the large increase in soil efflux
5 following rain (Fig. S1, Table 2).

6 The theoretical expectation for fully diffusive mixing between the CO_2 produced by
7 respiration and forest air was supported by most of the observations from the chambers, but
8 not all of the gas wells (Fig. 6). The lower line shows a Keeling-type regression for the soil
9 chamber inlets (Keeling, 1958). The intercept of the regression is shown, and represents the
10 $\delta^{13}C$ of the CO_2 added to forest air by soil respiration. This mixing occurs in the air above the
11 soil via turbulence that dominates transport over diffusion by several orders of magnitude. A
12 visual inspection of the chamber outlet data (Fig. 6) suggests that the data fall on the same
13 mixing line, which would be an indication that the soil chambers did not cause appreciable
14 perturbation to the diffusive efflux from the soil surface. The regression coefficients for the
15 chamber inlet and outlet data were slightly but significantly different due to the large sample
16 size examined here (Table 3). This conclusion was robust whether using the Keeling mixing
17 line as above or the Miller-Tans variant (Miller and Tans, 2003). The intercepts of
18 regressions using the chamber outlet data were enriched relative to the inlet regression
19 intercepts by $0.07 \pm 0.24\%$ to $0.59 \pm 0.15\%$, depending on which chamber or which method
20 was examined (Table 3). This was likely caused by a small perturbation to the diffusive flux
21 within the chamber while chamber CO_2 increased during measurement. Regardless, this
22 perturbation was minor relative to the diffusive enrichment within the soil. The theoretical
23 expectation for fully diffusive mixing between the CO_2 produced by respiration (square) and
24 forest air (circle) is shown by the solid line in Fig. 6. At depth (10 and 30 cm), the gas well
25 measurements conformed well to theory. At the O/A interface, the data fell well below the
26 expected diffusive mixing line. The 5 cm depth was intermediate between these.

27 Depth profiles of CO_2 and $\delta^{13}C$ of CO_2 are shown in Fig. 7 for the dry and moist periods, and
28 compared with best-fit diffusion model results. In general the profiles conformed to model
29 results, except for the shallow measurement depths (especially visible at the O/A interface in
30 Fig. 7 b, d). There was diel temporal variability in CO_2 and $\delta^{13}C$ of CO_2 (Fig. 4), but the diel
31 changes were minor relative to changes with depth (Fig. 7). Following rain, there was a
32 systematic and sustained increase in CO_2 at all depths (Fig. 7 a and c), which was concomitant

1 with increased soil efflux (Figs. 3, S1). The $\delta^{13}\text{C}$ of CO_2 is generally nonlinearly related to
2 CO_2 in the soil, and at higher CO_2 there is only a small change expected in $\delta^{13}\text{C}$ (see Fig. 5 in
3 Bowling et al., 2009). This is consistent with little change observed following rain in $\delta^{13}\text{C}$ of
4 CO_2 in the soil pore space (δ_{S} , Fig. 7 b, d). Neither the $\delta^{13}\text{C}$ of the soil efflux (δ_{R} , measured
5 with chambers), nor the $\delta^{13}\text{C}$ of production within the soil (δ_{J} , calculated from gas well data)
6 changed between the dry and moist periods (Fig. 7 b, d, Table 4). The $\delta^{13}\text{C}$ of CO_2 in the soil
7 pore space was always more enriched than the $\delta^{13}\text{C}$ of soil efflux (δ_{R}) or production within
8 the soil (δ_{J}), and especially so closer to the surface.

9 The δ_{J} varied systematically with depth, and at 10 and 30 cm was very close to δ_{R} as expected
10 from diffusion theory (Davidson, 1995, shading in Fig. 7 b, d). Note, however, that δ_{R} and δ_{J}
11 were statistically distinguishable in most cases (Table 4). The $\delta^{13}\text{C}$ of CO_2 in the soil pore
12 space was more enriched than expected based on best-fit diffusion model results at the O/A
13 interface (compare to model lines in Fig. 7b,d). This was true when model results were
14 compared to all measurement depths (solid line) or (dashed) excluding the O/A interface (0
15 cm). The δ_{J} at 5 cm and especially at the O/A interface were more negative than the $\delta^{13}\text{C}$ of
16 the soil efflux. This pattern was maintained for the full duration of the study. Frequency
17 distributions of all measurements of δ_{R} and δ_{J} are shown in Fig. 8. There was much higher
18 variability in δ_{R} than in δ_{J} , but this variability was not related to any measured environmental
19 parameters.

20 The mean $\delta^{13}\text{C}$ of soil efflux measured with the chambers was very similar to the mean
21 signature of whole-forest respiration (δ_{F} , Fig. 8, Bowling et al. 2014). The δ_{R} was very
22 similar to the mean δ_{J} at 5, 10, and 30 cm, but not at the O/A interface, whose distribution was
23 highly negatively skewed (Fig 8). The mean δ_{R} and δ_{J} at depth differed minimally but the
24 differences were statistically significant due to the large number of samples (Table 4). This
25 pattern was observed for the full data set (Fig. 8) and also during the dry and moist periods
26 (Table 4). In all cases the soil efflux δ_{R} was only a small amount (0.4 to 0.6 ‰) enriched
27 relative to δ_{J} at 10 and 30 cm depth (Table 4). Due to the large number of samples, we do not
28 interpret these small statistical differences as providing particularly meaningful information
29 about ecological processes, with the exception of the O/A interface and 5 cm depths (as will
30 be discussed later).

31

1 **4 Discussion**

2 Biological respiration is highly responsive to temperature (Davidson and Janssens, 2006), and
3 it is well-established that the process rate of respiration and the soil efflux both vary with
4 temperature on diel (Savage et al., 2013) and seasonal (Jassal et al., 2005) time scales. Our
5 observations of soil efflux and soil temperature also showed correlated diel variability as
6 expected (Figs. 3, 5, S1). Several studies have reported diel variation in the $\delta^{13}\text{C}$ of the soil
7 efflux (Bahn et al., 2009; Kodama et al., 2008; Marron et al., 2009), but in our case there was
8 no diel variation in the $\delta^{13}\text{C}$ of soil respiration (neither δ_{R} , Fig. 5 nor δ_{J} , Fig. 7). The potential
9 biological mechanisms that would lead to diel variation in $\delta^{13}\text{C}$ of respiration have been
10 recently reviewed (Werner and Gessler, 2011), and include variation in respiratory substrate,
11 isotopic fractionation, and/or changes in relative amounts of component fluxes such as
12 autotrophic (rhizospheric) and heterotrophic respiration. There is compelling evidence for a
13 short-term linkage between photosynthesis and belowground respiration (Kuzyakov and
14 Gavrichkova, 2010), almost certainly mediated by the roots and their symbionts (Hopkins et
15 al., 2013; Savage et al., 2013). Several studies have highlighted isotopic signals in respiration
16 from the soil or whole forests that appear to be influenced by photosynthetic response to
17 humidity or water availability (see reviews by Bowling et al., 2008; Brüggemann et al., 2011),
18 which might be expected to lead to diel changes in $\delta^{13}\text{C}$ of soil efflux. However, purely
19 physical processes of heat conduction and diffusive transport can also lead to diel variability
20 in soil efflux rate and its time-lagged correlation with soil temperature (Phillips et al., 2011),
21 and in the $\delta^{13}\text{C}$ of soil respiration (Bowling et al., 2011; Moyes et al., 2010). To date these
22 physical processes have been under-appreciated by the soil ecological community. It is
23 possible that strictly biological interpretations of diel variation in $\delta^{13}\text{C}$ of soil respiration are
24 too simplistic. Based on these results we reject our first hypothesis – there appears to be no
25 diel variation in $\delta^{13}\text{C}$ of soil efflux at our study forest. We cannot explain why others have
26 found such variation and we have not.

27 Rainfall wets the soil from the top down, and in previously dry soils can markedly increase
28 overall respiration rate (Borken and Matzner, 2009). Presumably this effect is dominated by
29 heterotrophic activity, with changes in microbial community composition and function (Fierer
30 et al., 2003; Placella et al., 2012), but the rhizosphere (and rhizosphere symbionts) can
31 respond to wetting as well. This may lead to priming of decomposition and nutrient
32 mineralization (Dijkstra and Cheng, 2007) as well as enhanced activity by root symbionts

1 (Querejeta et al., 2003). Such processes can be directly mediated via plant roots. For
2 example, watering soil on only one side of a ponderosa pine tree enhances soil CO₂ efflux on
3 the dry side (Irvine et al., 2005).

4 There are no known general patterns for carbon isotopic response to wetting in the soil CO₂
5 efflux. Immediate effects of rain involve decreased gas diffusivity and solubilisation of
6 existing pore space CO₂ in water (Gamnitzer et al., 2011), and after hours to days, changes in
7 biological processes as described above. All might be expected to have isotopic effects.
8 Wingate and colleagues (2010) found in a maritime pine forest that $\delta^{13}\text{C}$ of the soil efflux
9 varied slowly over several months by ~ 2 ‰, becoming most enriched in midsummer, but
10 there was no clear change following frequent wetting events. A root exclusion experiment
11 demonstrated that there is minimal variability in $\delta^{13}\text{C}$ of microbial respiration, but variability
12 in $\delta^{13}\text{C}$ of autotrophic respiration related to drought, possibly implicating photosynthesis
13 (Risk et al., 2012). Lab incubation experiments have shown no change in $\delta^{13}\text{C}$ of
14 heterotrophic respiration over a broad moisture range (Phillips et al., 2010). In some semi-arid
15 ecosystems rain pulses and irrigation experiments have led to 6-8 ‰ isotopic changes (both
16 enrichment and depletion) in $\delta^{13}\text{C}$ of soil efflux (Powers et al., 2010; Unger et al., 2012). In
17 our case, there was no change in δ_R or δ_J over two months despite several occurrences of rain
18 (Figs. 3, 7). The first rain event shown increased the soil efflux by up to 39 % (Table 3, Fig.
19 3), so it is highly likely that heterotrophic respiration increased. The $\delta^{13}\text{C}$ of the soil efflux
20 was highly variable but δ_J was quite consistent and the means of both measures were nearly
21 invariant over the study (Fig. 8). Hence there appears to be no generalizable pattern in the
22 $\delta^{13}\text{C}$ of soil efflux following wetting, and we reject our second hypothesis. We do not know
23 why others have found such high variation in $\delta^{13}\text{C}$ of soil efflux in response to wetting while
24 we did not.

25 Several studies have interpreted variation in isotope content of soil respiration in the context
26 of partitioning autotrophic and heterotrophic respiration (see reviews by Kuzyakov, 2006;
27 Paterson et al., 2009). It is certain that both respiratory processes were occurring in our
28 system, but there was no diel change in δ_R or δ_J (Figs. 5, 7), and no change in either following
29 rain. Isotopic transformations of carbon in the plant-soil-microbial system are quite complex
30 (Brüggemann et al., 2011) and often the isotopic difference in autotrophic and heterotrophic
31 respiration is too small to be useful in partitioning between them (Formánek and Ambus,
32 2004; Kuzyakov, 2006). These results suggest that natural abundance carbon isotope studies

1 in C3 ecosystems are not likely to be a generally useful tool for partitioning of soil
2 respiration. We recommend that future isotopic studies focused on partitioning the
3 components of soil respiration take advantage of recent major advances in isotopic labelling
4 (Carbone et al., 2007; Epron et al., 2012; Hogberg et al., 2008).

5 Several studies have shown that trace gas transport in porous soils in a variety of ecosystems
6 is subject to ventilation by wind or pressure pumping (e.g., Flechard et al., 2007; Fujiyoshi et
7 al., 2010; Maier et al., 2010; Sánchez-Cañete et al., 2013), and even by thermal convection
8 (Ganot et al., 2014). When diffusion initially dominates transport and a ventilation event
9 follows, there should be a readily detectible isotopic effect as ventilation removes some of the
10 small pool of diffusively-enriched CO₂ within the soil (as described in Fig. 1). We have
11 previously reported the isotopic effect of ventilation within the snowpack at the Niwot Ridge
12 forest (Bowling and Massman, 2011). In that study, a sustained wind event decreased the
13 CO₂ within the upper soil by 30 % (1000 μmol mol⁻¹ decrease), even though the soil was
14 covered by a ~1m deep snowpack. The bulk fluid flow likely penetrates only a few cm into
15 the surface of a snowpack (Clifton et al., 2008), but trace gas mole fractions can change
16 substantially deeper following the perturbation to diffusion (Seok et al., 2009). For these
17 reasons we anticipated that in summer, without the physical barrier of a snowpack, the
18 isotopic effect of ventilation within soils would be quite strong.

19 Passage of weather systems in our study led to expected variation in barometric pressure and
20 wind speed (Fig. 4), with concomitant variation in soil CO₂ as deep as 30 cm (Fig. 4).
21 However, the variability in soil CO₂ was fairly minor (compare Fig. 4 to dramatic changes in
22 Fig. 3 of Sánchez-Cañete et al., 2013) and soil CO₂ was not correlated with wind speed,
23 friction velocity, or pressure. Large changes in soil CO₂ were related to rain events (Fig. 3) as
24 gas diffusivity of the bulk soil system changed with soil moisture content. There were no
25 discernible isotopic effects associated with pressure variation (not shown, but note the very
26 limited variation in δ_R, δ_S and δ_J over the full experiment in Fig. 7, and adherence of 10 and
27 30 cm depths to the upper (diffusive) mixing line in Fig. 6). Hence, we find no isotopic
28 evidence for pressure-induced ventilation of the deep soil (10 cm or greater below the O/A
29 interface) in summer at the Niwot Ridge forest, and thus reject our third hypothesis (but with
30 a caveat that will be discussed later).

31 This result contrasts directly with observations under the snowpack at the same forest
32 (Bowling and Massman, 2011), where large (30%) changes in CO₂ in the upper soil were

1 caused by wind. This can be explained by considering the medium directly above the soil
2 surface as a boundary condition for the soil diffusive system. Due to the high permeability of
3 the snowpack, wind perturbations to the diffusive gradient cause large changes in CO₂ just
4 above the soil surface (at the bottom of the snowpack). In summer, even though CO₂ does
5 change in forest air above the soil, this variation is minor relative to the vertical gradient in
6 CO₂ within the soil (Fig 7a,b), and so wind does not affect the soil surface boundary condition
7 appreciably. This result, of course, is dependent on the magnitude of the total production of
8 CO₂. At very low production rates, variability in forest air CO₂ at the soil surface would be
9 much larger relative to the smaller vertical gradients associated with low production. This
10 physical effect can influence diffusion to markedly affect diel variation in the $\delta^{13}\text{C}$ of the soil
11 gas system (Bowling et al., 2011; Moyes et al., 2010).

12 Our study confirms theoretical expectations of gas transport in the biophysical soil system,
13 but also highlights a limitation of diffusion-only models in the context of experimentally-
14 induced advection. A very important aspect of existing theory asserts that at steady state the
15 $\delta^{13}\text{C}$ of soil efflux matches the $\delta^{13}\text{C}$ of biological production, but both differ from the $\delta^{13}\text{C}$ of
16 CO₂ within the soil (Cerling et al., 1991; Davidson, 1995). Our results are in agreement –
17 extensive measurements of δ_{R} using soil chambers were consistent with those of δ_{J} from gas
18 wells at the 10 and 30 cm depths, over the entire 2-month study ($n > 1000$ in each case, Fig.
19 8). These observations of δ_{R} and δ_{J} also match the $\delta^{13}\text{C}$ of whole-forest respiration obtained
20 from measurements of forest air (Fig. 8 top panel), providing confidence that the entire gas
21 transport system is primarily diffusive and well described by present theoretical
22 understanding.

23 However, the δ_{J} observed at the O/A interface, and at 5 cm depth, were both more negative
24 than δ_{R} (Figs. 7, 8, Table 4). There are two possible ways to interpret this difference. First,
25 natural ventilation of the near surface soils by wind/pressure could cause mixing of CO₂ in the
26 profile with CO₂ in air, which would decrease CO₂ and make $\delta^{13}\text{C}$ of CO₂ less negative at the
27 O/A interface and the 5 cm depth. This is consistent with observations of C_{S} and δ_{S} (black
28 boxes in Fig. 7), and with the deviation away from the upper diffusive line (Fig. 6) at these
29 depths. However, if persistent natural ventilation were occurring, the δ_{R} measured
30 independently using the chambers (purple in Fig. 7) would match δ_{J} at the O/A interface,
31 since that gas diffuses directly into the chambers – but this did not occur. Hence a second
32 interpretation is most likely correct: pumping of gas from the shallower soil gas wells to

1 transport it to the analyser caused artificial mixing of forest air with soil air by advection.
2 Observations of δ_j from the 10 and 30 cm depths matched δ_R from the chambers (Figs. 7, 8)
3 and the mixing at these depths was consistent with diffusion theory (Figs. 1, 6) and best-fit
4 diffusion model results (Fig. 7). Mixing of gas at these depths due to pumping likely
5 occurred, but the vertical gradients of CO₂ and especially $\delta^{13}\text{C}$ of CO₂ (Fig. 7) were much
6 smaller at these depths, and thus δ_j was not affected. Future studies that seek to examine the
7 near-surface influence of atmospheric turbulence on soil gas transport must strive to minimize
8 artefacts due to sampling. This could be facilitated by minimizing the amount of soil gas
9 required for sampling (Moyes and Bowling, 2013), or a sampling design which allows a
10 larger soil volume to be sampled without disturbance to diffusion (e.g., Parent et al., 2013).

11 The $\delta^{13}\text{C}$ of the soil efflux measured in chambers was considerably more variable than the
12 $\delta^{13}\text{C}$ of production observed using the gas wells (Fig. 8), but their means were quite similar.
13 The soil efflux was roughly normally distributed, but at depth the distributions for δ_j were
14 more peaked (high kurtosis). We examined a number of possible reasons to explain the
15 higher variability in $\delta^{13}\text{C}$ of the soil efflux. We could find no relation between variability of
16 δ_R and statistical metrics (mean, variance, rate of change, friction velocity) of wind speed or
17 barometric pressure. Variability was also unrelated to sunlight, humidity, soil temperature,
18 soil moisture, soil efflux, and CO₂ mole fraction increase during chamber closure. This
19 contrasts with other studies that have shown correlations between soil CO₂ and/or soil efflux
20 with these environmental forcing mechanisms (e.g., Davidson et al., 1998; Roland et al.,
21 2015; Sánchez-Cañete et al., 2013; Savage et al., 2013; Subke et al., 2003), highlighting the
22 variability in these processes across the landscape.

23 The $\delta^{13}\text{C}$ of soil air in upper horizons is susceptible to advection due to natural weather
24 dynamics and to methodological artifacts. Using alternative methods Goffin and colleagues
25 (2014) showed that $\delta^{13}\text{C}$ of CO₂ in a highly permeable litter layer was indeed affected by
26 turbulence. Given our pumping artefact, we cannot exclude the possibility of pressure-
27 induced transport near the soil surface using our gas well data. In fact, the much higher
28 variability in $\delta^{13}\text{C}$ of soil efflux relative to δ_j from the gas wells at 10 and 30 cm depths (Fig.
29 8) may provide evidence for pressure-induced variation in gas transport near the surface.
30 Shearing of wind by forest canopy elements induces variability in magnitude and spectral
31 composition of wind velocity and momentum flux with length scales of similar size to the
32 spacing of canopy elements (Amiro, 1990; Tóta et al., 2012; Vickers and Thomas, 2014).

1 This is likely to induce pressure variation within the soil with similar horizontal length scales
2 that varies with wind speed, direction, and surface roughness (Albert and Hawley, 2002;
3 Baldocchi and Meyers, 1991; Staebler and Fitzjarrald, 2005). Conservation of mass requires
4 that on average δ_R should match δ_J (as it does at 10 and 30 cm depths, Fig. 8), but the
5 presence of such dynamic fluid forcing could lead to transient spatial variability in $\delta^{13}\text{C}$ of
6 efflux measured in the chambers (as observed with higher variability in δ_R than δ_J). Hence we
7 cannot fully reject our third hypothesis, which states that pressure variation leads to
8 ventilation of the soil. We have shown strong evidence that ventilation does not occur at 10
9 and 30 cm depths, but our data cannot exclude the possibility of ventilation of the shallower
10 soil.

11

12 **5 Conclusions**

13 We have examined the isotopic composition of CO_2 produced by respiration of soil organisms
14 with an extensive data set utilizing three independent methods – soil surface chambers, soil
15 pore gas wells, and forest air inlets – and compared these results with a steady state diffusion
16 model. Results were consistent between the three methods and conformed well to physical
17 theory of diffusive transport in soils. This concordance provides strong evidence that
18 experimental artefacts associated with chamber-soil pressure gradients were absent in our soil
19 chambers. However, we have shown that more negative values for the $\delta^{13}\text{C}$ of CO_2 produced
20 within the soil that were derived from shallower soil pore measurements were inconsistent
21 with best-fit diffusion model results and with soil chamber observations, and thus must have
22 been artificially induced by pumping.

23 From these observations we reject two of our three hypotheses. We found no evidence for
24 diel variation in the $\delta^{13}\text{C}$ of the soil efflux or of the CO_2 produced within the soil. We found
25 no evidence that rain leads to changes in $\delta^{13}\text{C}$ of the soil efflux. We were unable to explain
26 why others have found these patterns while we did not. Pressure-induced ventilation of the
27 soil did not occur at our deepest soil gas measurement depths, but the high variability of $\delta^{13}\text{C}$
28 of the soil efflux relative to CO_2 produced at depth suggests that there may be sporadic
29 ventilation at the shallower depths. We note that our results contrast with several other
30 studies, which demonstrate that there is high variability in biophysical forcing of soil gas
31 transport across Earth's surface.

1 This study provides evidence that natural abundance carbon isotopes in C₃ ecosystems are not
2 a generally useful tool for partitioning of autotrophic and heterotrophic respiration, in
3 agreement with earlier studies (Formánek and Ambus, 2004; Kuzyakov, 2006). We
4 recommend that future isotopic studies that seek to disentangle the components of soil
5 respiration take advantage of powerful recent advances in isotopic labelling (Carbone et al.,
6 2007; Epron et al., 2012; Hogberg et al., 2008).

7

8

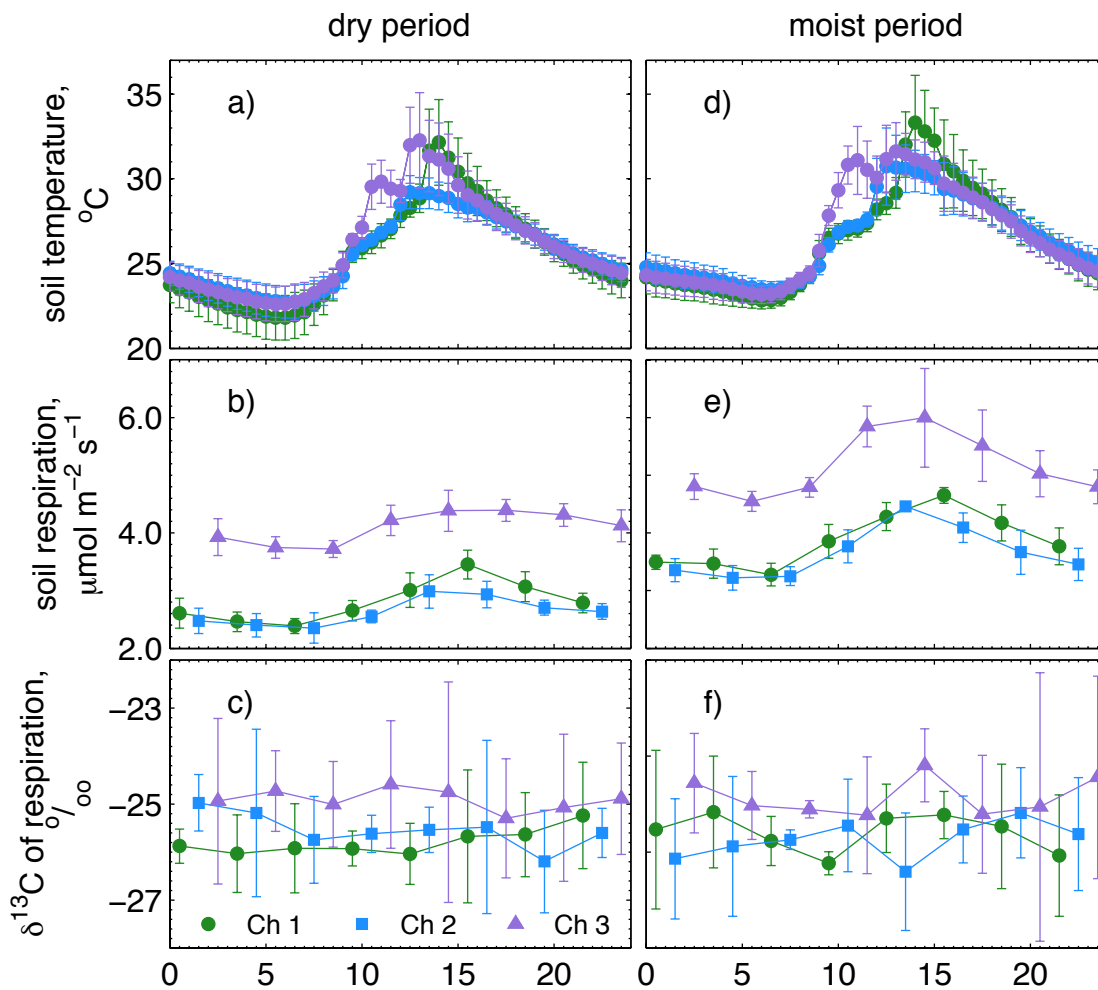
1 **Author Contributions**

2 D. B. designed the experiments, built the instrumentation and made the measurements. J. E.
3 conducted soil gas transport modeling, and S. H. performed statistical analyses. All co-
4 authors were active in scientific interpretation. D. B. prepared the manuscript with
5 contributions from co-authors.

6

7

8 **Appendix A**



9

10 Figure A1. Mean (5-day) diel patterns of soil temperature (5 cm), soil surface flux, and δ¹³C
11 of soil surface flux (δ_R) during the dry (left) and moist (right) periods. Data are shown for
12 chambers 1, 2, and 3 separately (legend in c). Normalized versions of these plots are shown
13 in Fig. 5 of the main article.

1

2 **Acknowledgements**

3 All data from this study are available for collaborative use by anyone interested; contact D. B.
4 for information on data access (david.bowling@utah.edu). Thanks to J. Knowles and A.
5 Chan for outstanding field assistance, to N. Nickerson and T. Huth for help with modeling, to
6 T. Cerling and G. Maurer for several thoughtful discussions, to L. Wingate for loaning a
7 prototype soil chamber, and to E. Grote for helping with chamber automation. We are
8 grateful to S. Burns and P. Blanken for providing weather data from the Niwot AmeriFlux
9 tower. This work was supported by the U.S. Department of Energy, Office of Science, Office
10 of Biological and Environmental Research, Terrestrial Ecosystem Science Program under
11 Award Numbers DE-SC0005236 and DE-SC0010625. D. B. and S. H. were also supported
12 by NSF EPSCoR grant EPS 1208732 awarded to Utah State University, as part of the State of
13 Utah EPSCoR Research Infrastructure Improvement Award. J. E. is grateful for additional
14 support from a Research-in-Residence Award from the Inter-university Training in
15 Continental-scale Ecology Project, NSF EF-1137336.

16

17

1 **References**

- 2 Albert, M. R. and Hawley, R. L.: Seasonal changes in snow surface roughness characteristics
3 at Summit, Greenland: implications for snow and firn ventilation, *Ann. Glaciol.*, 35, 510–514,
4 2002.
- 5 Amiro, B. D.: Drag coefficients and turbulence spectra within three boreal forest canopies,
6 *Bound.-Layer Meteorol.*, 52(3), 227–246, doi:10.1007/BF00122088, 1990.
- 7 Amundson, R., Stern, L., Baisden, T. and Wang, Y.: The isotopic composition of soil and
8 soil-respired CO₂, *Geoderma*, 82(1-3), 83–114, 1998.
- 9 Angert, A., Yakir, D., Rodeghiero, M., Preisler, Y., Davidson, E. A. and Weiner, T.: Using
10 O₂ to study the relationships between soil CO₂ efflux and soil respiration, *Biogeosciences*,
11 12(7), 2089–2099, doi:10.5194/bg-12-2089-2015, 2015.
- 12 Aubrey, D. P. and Teskey, R. O.: Root-derived CO₂ efflux via xylem stream rivals soil CO₂
13 efflux, *New Phytol.*, 184(1), 35–40, 2009.
- 14 Bahn, M., Schmitt, M., Siegwolf, R., Richter, A. and Brüggemann, N.: Does photosynthesis
15 affect grassland soil-respired CO₂ and its carbon isotope composition on a diurnal timescale?,
16 *New Phytol.*, 182(2), 451–460, 2009.
- 17 Baldocchi, D. D. and Meyers, T. P.: Trace gas exchange above the floor of a deciduous forest
18 1. Evaporation and CO₂ efflux, *J. Geophys. Res.*, 96(D4), 7271–7285, 1991.
- 19 Ballantyne, A. P., Miller, J. B., Baker, I. T., Tans, P. P. and White, J. W. C.: Novel
20 applications of carbon isotopes in atmospheric CO₂: What can atmospheric measurements
21 teach us about processes in the biosphere?, *Biogeosciences*, 8(10), 3093–3106, 2011.
- 22 Bardgett, R. D., Freeman, C. and Ostle, N. J.: Microbial contributions to climate change
23 through carbon cycle feedbacks, *ISME J.*, 2(8), 805–814, doi:10.1038/ismej.2008.58, 2008.
- 24 Bird, J. A. and Torn, M. S.: Fine roots vs. Needles: A comparison of C-13 and N-15 dynamics
25 in a ponderosa pine forest soil, *Biogeochemistry*, 79(3), 361–382, 2006.
- 26 Borken, W. and Matzner, E.: Reappraisal of drying and wetting effects on C and N
27 mineralization and fluxes in soils, *Glob. Change Biol.*, 15(4), 808–824, doi:10.1111/j.1365-
28 2486.2008.01681.x, 2009.
- 29 Bowling, D. R. and Massman, W. J.: Persistent wind-induced enhancement of diffusive CO₂
30 transport in a mountain forest snowpack, *J. Geophys. Res.*, 116, 15 PP.,
31 doi:201110.1029/2011JG001722, 2011.
- 32 Bowling, D. R., Pataki, D. E. and Randerson, J. T.: Carbon isotopes in terrestrial ecosystem
33 pools and CO₂ fluxes, *New Phytol.*, 178, 24–40, doi: 10.1111/j.1469–8137.2007.02342.x,
34 2008.
- 35 Bowling, D. R., Massman, W. J., Schaeffer, S. M., Burns, S. P., Monson, R. K. and Williams,
36 M. W.: Biological and physical influences on the carbon isotope content of CO₂ in a

- 1 subalpine forest snowpack, Niwot Ridge, Colorado, *Biogeochemistry*, 95(1), 37–59,
2 doi:10.1007/s10533-008-9233-4, 2009.
- 3 Bowling, D. R., Grote, E. E. and Belnap, J.: Rain pulse response of soil CO₂ exchange by
4 biological soil crusts and grasslands of the semiarid Colorado Plateau, United States, *J.*
5 *Geophys. Res. G Biogeosciences*, 116(3) [online] Available from:
6 [http://www.scopus.com/inward/record.url?eid=2-s2.0-](http://www.scopus.com/inward/record.url?eid=2-s2.0-80052703983&partnerID=40&md5=09638013fb435de41921c8024fb74fd9)
7 [80052703983&partnerID=40&md5=09638013fb435de41921c8024fb74fd9](http://www.scopus.com/inward/record.url?eid=2-s2.0-80052703983&partnerID=40&md5=09638013fb435de41921c8024fb74fd9), 2011.
- 8 Bowling, D. R., Ballantyne, A. P., Miller, J. B., Burns, S. P., Conway, T. J., Menzer, O.,
9 Stephens, B. B. and Vaughn, B. H.: Ecological processes dominate the ¹³C land
10 disequilibrium in a Rocky Mountain subalpine forest, *Glob. Biogeochem. Cycles*, 28(4),
11 2013GB004686, doi:10.1002/2013GB004686, 2014.
- 12 Brüggemann, N., Gessler, A., Kayler, Z., Keel, S. G., Badeck, F., Barthel, M., Boeckx, P.,
13 Buchmann, N., Brugnoli, E., Esperschütz, J., Gavrichkova, O., Ghashghaie, J., Gomez-
14 Casanovas, N., Keitel, C., Knohl, A., Kuptz, D., Palacio, S., Salmon, Y., Uchida, Y. and
15 Bahn, M.: Carbon allocation and carbon isotope fluxes in the plant-soil-atmosphere
16 continuum: A review, *Biogeosciences*, 8(11), 3457–3489, 2011.
- 17 Carbone, M. S., Czimczik, C. I., McDuffee, K. E. and Trumbore, S. E.: Allocation and
18 residence time of photosynthetic products in a boreal forest using a low-level ¹⁴C pulse-chase
19 labeling technique, *Glob. Change Biol.*, 13(2), 466–477, 2007.
- 20 Cerling, T. E.: The stable isotopic composition of modern soil carbonate and its relationship
21 to climate, *Earth Planet. Sci. Lett.*, 71, 229–240, 1984.
- 22 Cerling, T. E., Solomon, D. K., Quade, J. and Bowman, J. R.: On the isotopic composition of
23 carbon in soil carbon dioxide, *Geochim. Cosmochim. Acta*, 55, 3403–3405, 1991.
- 24 Clifton, A., Manes, C., Ruedi, J. D., Guala, M. and Lehning, M.: On shear-driven ventilation
25 of snow, *Bound.-Layer Meteorol.*, 126, 249–261, 2008.
- 26 Cole, J. C. and Braddock, W. A.: Geologic Map of the Estes Park 30' x 60' Quadrangle,
27 North-Central Colorado, USGS Scientific Investigations Map 3039, U.S. Geological Survey.,
28 2009.
- 29 Conant, R. T., Ryan, M. G., Ågren, G. I., Birge, H. E., Davidson, E. A., Eliasson, P. E.,
30 Evans, S. E., Frey, S. D., Giardina, C. P., Hopkins, F. M., Hyvönen, R., Kirschbaum, M. U.
31 F., Lavallee, J. M., Leifeld, J., Parton, W. J., Megan Steinweg, J., Wallenstein, M. D., Martin
32 Wetterstedt, J. Å. and Bradford, M. A.: Temperature and soil organic matter decomposition
33 rates – synthesis of current knowledge and a way forward, *Glob. Change Biol.*, 17(11), 3392–
34 3404, doi:10.1111/j.1365-2486.2011.02496.x, 2011.
- 35 Davidson, E. A. and Janssens, I. A.: Temperature sensitivity of soil carbon decomposition and
36 feedbacks to climate change, *Nature*, 440(7081), 165–173, 2006.
- 37 Davidson, E. A., Belk, E. and Boone, R. D.: Soil water content and temperature as
38 independent or confounded factors controlling soil respiration in a temperate mixed hardwood
39 forest, *Glob. Change Biol.*, 4(2), 217–227, 1998.

- 1 Davidson, G. R.: The stable isotopic composition and measurement of carbon in soil CO₂,
2 *Geochim. Cosmochim. Acta*, 59(12), 2485–2489, doi:10.1016/0016-7037(95)00143-3, 1995.
- 3 Dijkstra, F. A. and Cheng, W.: Interactions between soil and tree roots accelerate long-term
4 soil carbon decomposition, *Ecol. Lett.*, 10(11), 1046–1053, 2007.
- 5 Ekblad, A. and Högberg, P.: Natural abundance of ¹³C in CO₂ respired from forest soils
6 reveals speed of link between tree photosynthesis and root respiration, *Oecologia*, 127(3),
7 305–308, 2001.
- 8 Epron, D., Bahn, M., Derrien, D., Lattanzi, F. A., Pumpanen, J., Gessler, A., Högberg, P.,
9 Maillard, P., Dannoura, M., Gérant, D. and Buchmann, N.: Pulse-labelling trees to study
10 carbon allocation dynamics: a review of methods, current knowledge and future prospects,
11 *Tree Physiol.*, 32(6), 776–798, doi:10.1093/treephys/tps057, 2012.
- 12 Fang, C. and Moncrieff, J. B.: An open-top chamber for measuring soil respiration and the
13 influence of pressure difference on CO₂ efflux measurement, *Funct. Ecol.*, 12(2), 319–325,
14 1998.
- 15 Fierer, N., Schimel, J. P. and Holden, P. A.: Influence of drying-rewetting frequency on soil
16 bacterial community structure, *Microb. Ecol.*, 45(1), 63–71, 2003.
- 17 Flechard, C. R., Neftel, A., Jocher, M., Ammann, C., Leifeld, J. and Fuhrer, J.: Temporal
18 changes in soil pore space CO₂ concentration and storage under permanent grassland, *Agric.
19 For. Meteorol.*, 142, 66–84, 2007.
- 20 Formánek, P. and Ambus, P.: Assessing the use of $\delta^{13}\text{C}$ natural abundance in separation of
21 root and microbial respiration in a Danish beech (*Fagus sylvatica* L.) forest, *Rapid Commun.
22 Mass Spectrom.*, 18(8), 897–902, doi:10.1002/rcm.1424, 2004.
- 23 Friedlingstein, P., Meinshausen, M., Arora, V. K., Jones, C. D., Anav, A., Liddicoat, S. K.
24 and Knutti, R.: Uncertainties in CMIP5 Climate Projections due to Carbon Cycle Feedbacks,
25 *J. Clim.*, 27(2), 511–526, doi:10.1175/JCLI-D-12-00579.1, 2014.
- 26 Fujiyoshi, R., Haraki, Y., Sumiyoshi, T., Amano, H., Kobal, I. and Vaupotic, J.: Tracing
27 the sources of gaseous components (²²²Rn, CO₂ and its carbon isotopes) in soil air under a
28 cool-deciduous stand in Sapporo, Japan, *Environ. Geochem. Health*, 32, 73–82, 2010.
- 29 Gannitzer, U., Moyes, A. B., Bowling, D. R. and Schnyder, H.: Measuring and modeling the
30 isotopic composition of soil respiration: insights from a grassland tracer experiment,
31 *Biogeosciences*, 8, 1333–1350, 2011.
- 32 Ganot, Y., Dragila, M. I. and Weisbrod, N.: Impact of thermal convection on CO₂ flux across
33 the earth–atmosphere boundary in high-permeability soils, *Agric. For. Meteorol.*, 184, 12–24,
34 doi:10.1016/j.agrformet.2013.09.001, 2014.
- 35 Ghashghaie, J. and Badeck, F. W.: Opposite carbon isotope discrimination during dark
36 respiration in leaves versus roots – a review, *New Phytol.*, 201(3), 751–769,
37 doi:10.1111/nph.12563, 2014.

- 1 Goffin, S., Aubinet, M., Maier, M., Plain, C., Schack-Kirchner, H. and Longdoz, B.:
2 Characterization of the soil CO₂ production and its carbon isotope composition in forest soil
3 layers using the flux-gradient approach, *Agric. For. Meteorol.*, 188, 45–57,
4 doi:10.1016/j.agrformet.2013.11.005, 2014.
- 5 Heimann, M. and Reichstein, M.: Terrestrial ecosystem carbon dynamics and climate
6 feedbacks, *Nature*, 451(7176), 289–292, doi:10.1038/nature06591, 2008.
- 7 Högberg, P., Nordgren, A., Buchmann, N., Taylor, A. F. S., Ekblad, A., Högberg, M. N.,
8 Nyberg, G., Ottosson-Lofvenius, M. and Read, D. J.: Large-scale forest girdling shows that
9 current photosynthesis drives soil respiration, *Nature*, 411, 789–792, 2001.
- 10 Hogberg, P., Hogberg, M. N., Gottlicher, S. G., Betson, N. R., Keel, S. G., Metcalfe, D. B.,
11 Campbell, C., Schindlbacher, A., Hurry, V., Lundmark, T., Linder, S. and Nasholm, T.: High
12 temporal resolution tracing of photosynthate carbon from the tree canopy to forest soil
13 microorganisms, *New Phytol.*, 177(1), 220–228, 2008.
- 14 Hopkins, F., Gonzalez-Meler, M. A., Flower, C. E., Lynch, D. J., Czimczik, C., Tang, J. and
15 Subke, J.-A.: Ecosystem-level controls on root-rhizosphere respiration, *New Phytol.*, 199(2),
16 339–351, doi:10.1111/nph.12271, 2013.
- 17 Irvine, J., Law, B. E. and Kurpius, M. R.: Coupling of canopy gas exchange with root and
18 rhizosphere respiration in a semi-arid forest, *Biogeochemistry*, 271–282, 2005.
- 19 Jarvis, P., Rey, A., Petsikos, C., Wingate, L., Rayment, M., Pereira, J., Banza, J., David, J.,
20 Miglietta, F., Borghetti, M., Manca, G. and Valentini, R.: Drying and wetting of
21 Mediterranean soils stimulates decomposition and carbon dioxide emission: The “Birch
22 effect,” *Tree Physiol.*, 27(7), 929–940, 2007.
- 23 Jassal, R., Black, A., Novak, M., Morgenstern, K., Nestic, Z. and Gaumont-Guay, D.:
24 Relationship between soil CO₂ concentrations and forest-floor CO₂ effluxes, *Agric. For.*
25 *Meteorol.*, 130(3–4), 176–192, doi:10.1016/j.agrformet.2005.03.005, 2005.
- 26 Keeling, C. D.: The concentration and isotopic abundances of atmospheric carbon dioxide in
27 rural areas, *Geochim. Cosmochim. Acta*, 13(4), 322–334, 1958.
- 28 Kodama, N., Barnard, R., Salmon, Y., Weston, C., Ferrio, J., Holst, J., Werner, R., Saurer,
29 M., Rennenberg, H., Buchmann, N. and Gessler, A.: Temporal dynamics of the carbon
30 isotope composition in a *Pinus sylvestris* stand: from newly assimilated organic carbon to
31 respired carbon dioxide, *Oecologia*, 156(4), 737–750, 2008.
- 32 Kuzyakov, Y.: Sources of CO₂ efflux from soil and review of partitioning methods, *Soil Biol.*
33 *Biochem.*, 38(3), 425–448, doi:10.1016/j.soilbio.2005.08.020, 2006.
- 34 Kuzyakov, Y. and Gavrichkova, O.: REVIEW: Time lag between photosynthesis and carbon
35 dioxide efflux from soil: a review of mechanisms and controls, *Glob. Change Biol.*, 16(12),
36 3386–3406, doi:10.1111/j.1365-2486.2010.02179.x, 2010.
- 37 Lai, C.-T., Ehleringer, J. R., Schauer, A. J., Tans, P. P., Hollinger, D. Y., Paw U, K. T.,
38 Munger, J. W. and Wofsy, S. C.: Canopy-scale δ¹³C of photosynthetic and respiratory CO₂

- 1 fluxes: observations in forest biomes across the United States, *Glob. Change Biol.*, 11(4),
2 633–643, 2005.
- 3 Lewis, W. M., Jr. and Grant, M. C.: Changes in the Output of Ions from a Watershed as a
4 Result of the Acidification of Precipitation, *Ecology*, 60(6), 1093–1097,
5 doi:10.2307/1936955, 1979.
- 6 Lloyd, J. and Taylor, J. A.: On the temperature dependence of soil respiration, *Funct. Ecol.*, 8,
7 315–323, 1994.
- 8 Maier, M., Schack-Kirchner, H., Hildebrand, E. E. and Holst, J.: Pore-space CO₂ dynamics in
9 a deep, well-aerated soil, *Eur. J. Soil Sci.*, 61, 877–887, 2010.
- 10 Marron, N., Plain, C., Longdoz, B. and Epron, D.: Seasonal and daily time course of the ¹³C
11 composition in soil CO₂ efflux recorded with a tunable diode laser spectrophotometer
12 (TDLS), *Plant Soil*, 318(1-2), 137–151, 2009.
- 13 Miller, J. B. and Tans, P. P.: Calculating isotopic fractionation from atmospheric
14 measurements at various scales, *Tellus*, 55B, 207–214, 2003.
- 15 Monson, R. K., Turnipseed, A. A., Sparks, J. P., Harley, P. C., Scott-Denton, L. E., Sparks, K.
16 and Huxman, T. E.: Carbon sequestration in a high-elevation, subalpine forest, *Glob. Change*
17 *Biol.*, 8, 459–478, 2002.
- 18 Moyes, A. B. and Bowling, D. R.: Interannual variation in seasonal drivers of soil respiration
19 in a semi-arid Rocky Mountain meadow, *Biogeochemistry*, 113(1-3), 683–697,
20 doi:10.1007/s10533-012-9797-x, 2013.
- 21 Moyes, A. B., Gaines, S. J., Siegwolf, R. T. W. and Bowling, D. R.: Diffusive fractionation
22 complicates isotopic partitioning of autotrophic and heterotrophic sources of soil respiration,
23 *Plant Cell Environ.*, 33(11), 1804–1819, doi:10.1111/j.1365-3040.2010.02185.x, 2010.
- 24 Nickerson, N., Egan, J. and Risk, D.: Subsurface approaches for measuring soil CO₂
25 isotopologue flux: Theory and application, *J. Geophys. Res. Biogeosciences*, 2013JG002508,
26 doi:10.1002/2013JG002508, 2014.
- 27 Parent, F., Plain, C., Epron, D., Maier, M. and Longdoz, B.: A new method for continuously
28 measuring the $\delta^{13}\text{C}$ of soil CO₂ concentrations at different depths by laser spectrometry, *Eur.*
29 *J. Soil Sci.*, 64(4), 516–525, doi:10.1111/ejss.12047, 2013.
- 30 Paterson, E., Midwood, A. J. and Millard, P.: Through the eye of the needle: a review of
31 isotope approaches to quantify microbial processes mediating soil carbon balance, *New*
32 *Phytol.*, 184(1), 19–33, doi:10.1111/j.1469-8137.2009.03001.x, 2009.
- 33 Phillips, C. L., Nickerson, N., Risk, D., Kayler, Z. E., Andersen, C., Mix, A. and Bond, B. J.:
34 Soil moisture effects on the carbon isotope composition of soil respiration, *Rapid Commun.*
35 *Mass Spectrom.*, 24(9), 1271–1280, 2010.
- 36 Phillips, C. L., Nickerson, N., Risk, D. and Bond, B. J.: Interpreting diel hysteresis between
37 soil respiration and temperature, *Glob. Change Biol.*, 17, 515–527, 2011.

- 1 Placella, S. A., Brodie, E. L. and Firestone, M. K.: Rainfall-induced carbon dioxide pulses
2 result from sequential resuscitation of phylogenetically clustered microbial groups, *Proc. Natl.*
3 *Acad. Sci. U. S. A.*, 109(27), 10931–10936, 2012.
- 4 Powers, H. H., Hunt, J. E., Hanson, D. T. and McDowell, N. G.: A dynamic soil chamber
5 system coupled with a tunable diode laser for online measurements of $\delta^{13}\text{C}$, $\delta^{18}\text{O}$, and efflux
6 rate of soil-respired CO_2 , *Rapid Commun. Mass Spectrom.*, 24(3), 243–253,
7 doi:10.1002/rcm.4380, 2010.
- 8 Le Quéré, C., Andres, R. J., Boden, T., Conway, T., Houghton, R. A., House, J. I., Marland,
9 G., Peters, G. P., van der Werf, G. R., Ahlström, A., Andrew, R. M., Bopp, L., Canadell, J.
10 G., Ciais, P., Doney, S. C., Enright, C., Friedlingstein, P., Huntingford, C., Jain, A. K.,
11 Jourdain, C., Kato, E., Keeling, R. F., Klein Goldewijk, K., Levis, S., Levy, P., Lomas, M.,
12 Poulter, B., Raupach, M. R., Schwinger, J., Sitch, S., Stocker, B. D., Viovy, N., Zaehle, S. and
13 Zeng, N.: The global carbon budget 1959–2011, *Earth Syst. Sci. Data*, 5(1), 165–185,
14 doi:10.5194/essd-5-165-2013, 2013.
- 15 Querejeta, J. I., Egerton-Warburton, L. M. and Allen, M. F.: Direct nocturnal water transfer
16 from oaks to their mycorrhizal symbionts during severe soil drying, *Oecologia*, 134(1), 55–
17 64, 2003.
- 18 Raich, J. W. and Schlesinger, W. H.: The global carbon dioxide flux in soil respiration and its
19 relationship to vegetation and climate, *Tellus B*, 44(2), doi:10.3402/tellusb.v44i2.15428,
20 1992.
- 21 Rayment, M. B. and Jarvis, P. G.: An improved open chamber system for measuring soil CO_2
22 effluxes in the field, *J. Geophys. Res. Atmospheres*, 102(D24), 28779–28784, 1997.
- 23 Riggs, A. C., Stannard, D. I., Maestas, F. B., Karlinger, M. R. and Striegl, R. G.: Soil CO_2
24 flux in the Amargosa Desert, Nevada, during El Niño 1998 and La Niña 1999, *U. S. Geol.*
25 *Surv. Sci. Investig. Rep.* 2009-5061, 2009.
- 26 Risk, D., Nickerson, N., Phillips, C. L., Kellman, L. and Moroni, M.: Drought alters respired
27 $\delta^{13}\text{C}\text{CO}_2$ from autotrophic, but not heterotrophic soil respiration, *Soil Biol. Biochem.*, 50, 26–
28 32, doi:10.1016/j.soilbio.2012.01.025, 2012.
- 29 Roland, M., Vicca, S., Bahn, M., Ladreiter-Knauss, T., Schmitt, M. and Janssens, I. A.:
30 Importance of non-diffusive transport for soil CO_2 efflux in a temperate mountain grassland,
31 *J. Geophys. Res. Biogeosciences*, 2014JG002788, doi:10.1002/2014JG002788, 2015.
- 32 Sánchez-Cañete, E. P., Kowalski, A. S., Serrano-Ortiz, P., Pérez-Priego, O. and Domingo, F.:
33 Deep CO_2 soil inhalation / exhalation induced by synoptic pressure changes and atmospheric
34 tides in a carbonated semiarid steppe, *Biogeosciences*, 10(10), 6591–6600, doi:10.5194/bg-
35 10-6591-2013, 2013.
- 36 Savage, K., Davidson, E. A. and Tang, J.: Diel patterns of autotrophic and heterotrophic
37 respiration among phenological stages, *Glob. Change Biol.*, 19(4), 1151–1159, 2013.
- 38 Schaeffer, S. M., Miller, J. B., Vaughn, B. H., White, J. W. C. and Bowling, D. R.: Long-term
39 field performance of a tunable diode laser absorption spectrometer for analysis of carbon
40 isotopes of CO_2 in forest air, *Atmospheric Chem. Phys.*, 8, 5263–5277, 2008.

- 1 Scott-Denton, L. E., Sparks, K. L. and Monson, R. K.: Spatial and temporal controls of soil
2 respiration rate in a high-elevation, subalpine forest, *Soil Biol. Biochem.*, 35, 525–534, 2003.
- 3 Seok, B., Helmig, D., Williams, M. W., Liptzin, D., Chowanski, K. and Hueber, J.: An
4 automated system for continuous measurements of trace gas fluxes through snow: An
5 evaluation of the gas diffusion method at a subalpine forest site, Niwot Ridge, Colorado,
6 *Biogeochemistry*, 95, 95–113, 2009.
- 7 Sommerfeld, R. A., Musselman, R. C., Reuss, J. O. and Mosier, A. R.: Preliminary
8 measurements of CO₂ in melting snow, *Geophys. Res. Lett.*, 18(7), 1225–1228, 1991.
- 9 Staebler, R. M. and Fitzjarrald, D. R.: Measuring Canopy Structure and the Kinematics of
10 Subcanopy Flows in Two Forests, *J. Appl. Meteorol.*, 44(8), 1161–1179,
11 doi:10.1175/JAM2265.1, 2005.
- 12 Subke, J. A., Reichstein, M. and Tenhunen, J. D.: Explaining temporal variation in soil CO₂
13 efflux in a mature spruce forest in Southern Germany, *Soil Biol. Biochem.*, 35(11), 1467–
14 1483, 2003.
- 15 Tóta, J., Roy Fitzjarrald, D. and da Silva Dias, M. A. F.: Amazon Rainforest Exchange of
16 Carbon and Subcanopy Air Flow: Manaus LBA Site—A Complex Terrain Condition, *Sci.*
17 *World J.*, 2012, doi:10.1100/2012/165067, 2012.
- 18 Unger, S., Máguas, C., Pereira, J. S., David, T. S. and Werner, C.: Interpreting post-drought
19 rewetting effects on soil and ecosystem carbon dynamics in a Mediterranean oak savannah,
20 *Agric. For. Meteorol.*, 154-155, X9–18, 2012.
- 21 Vickers, D. and Thomas, C. K.: Observations of the scale-dependent turbulence and
22 evaluation of the flux–gradient relationship for sensible heat for a closed Douglas-fir canopy
23 in very weak wind conditions, *Atmos Chem Phys*, 14(18), 9665–9676, doi:10.5194/acp-14-
24 9665-2014, 2014.
- 25 Werner, C. and Gessler, A.: Diel variations in the carbon isotope composition of respired CO₂
26 and associated carbon sources: A review of dynamics and mechanisms, *Biogeosciences*, 8(9),
27 2437–2459, 2011.
- 28 Wingate, L., Ogee, J., Burlett, R., Bosc, A., Devaux, M., Grace, J., Loustau, D. and Gessler,
29 A.: Photosynthetic carbon isotope discrimination and its relationship to the carbon isotope
30 signals of stem, soil and ecosystem respiration, *New Phytol.*, 188(2), 576–589, 2010.
- 31 Xiong, Y., D’Atri, J. J., Fu, S., Xia, H. and Seastedt, T. R.: Rapid soil organic matter loss
32 from forest dieback in a subalpine coniferous ecosystem, *Soil Biol. Biochem.*, 43(12), 2450–
33 2456, 2011.
- 34 Xu, L. K., Furtaw, M. D., Madsen, R. A., Garcia, R. L., Anderson, D. J. and McDermitt, D.
35 K.: On maintaining pressure equilibrium between a soil CO₂ flux chamber and the ambient
36 air, *J. Geophys. Res.-Atmospheres*, 111(D8), D08S10, doi:10.1029/2005JD006435, 2006.

37

38

1 Table 1. List of symbols used.

Symbol	Description	Unit
C	CO ₂ mole fraction relative to dry air	μmol mol ⁻¹
C _a	CO ₂ in air above the soil	μmol mol ⁻¹
C _S	CO ₂ in soil pore space	μmol mol ⁻¹
D	soil gas diffusivity	m ² s ⁻¹
δ ¹³ C	stable (¹³ C/ ¹² C) isotope composition (relative to VPDB)	‰
δ _a	δ ¹³ C of CO ₂ in air above the soil	‰
δ _F	δ ¹³ C of whole forest respiration	‰
δ _J	δ ¹³ C of soil CO ₂ production, calculated using Eq. 1	‰
δ _R	δ ¹³ C of soil surface CO ₂ flux	‰
δ _S	δ ¹³ C of soil pore space CO ₂	‰
ε	model fit error metric	dimensionless
η	e-folding depth of soil production function	m
L	lower model depth boundary	m
λ	arbitrary parameter to constrain production to 0 to L	m
P(z,t)	biological production at depth z and time t	mol CO ₂ m ⁻³ s ⁻¹
P _o	total biological production integrated over full soil	mol CO ₂ m ⁻² s ⁻¹
ρ _a	molar density of air	mol air m ⁻³
t	time	sec
θ	air-filled porosity of soil	dimensionless
X	CO ₂ concentration in soil	mol CO ₂ m ⁻³
z	depth	m

2

3

1 Table 2. Statistics for soil temperature, soil surface flux, and $\delta^{13}\text{C}$ of soil efflux (δ_{R}) during
 2 the 5-day dry and moist periods shown in Fig. 3. Values are shown for each chamber location
 3 separately. SD = standard deviation, CV = coefficient of variation expressed as a percentage.
 4 Number of measurements was $n=40$ for all cases (8 measurements per day at each location).

	Location	Dry period			Moist period		
		Mean	SD	CV	Mean	SD	CV
soil temperature ($^{\circ}\text{C}$)	1	25.5	2.9	11.4	26.3	3.0	11.4
	2	25.6	2.1	8.2	26.4	2.4	9.1
	3	26.1	2.9	11.1	26.7	2.9	10.9
soil surface flux ($\mu\text{mol m}^{-2} \text{s}^{-1}$)	1	2.80	0.36	12.7	3.87	0.47	12.1
	2	2.63	0.23	8.9	3.66	0.44	11.9
	3	4.10	0.27	6.7	5.17	0.54	10.5
$\delta^{13}\text{C}$ of soil surface flux (δ_{R} , ‰)	1	-25.8	0.3	1.0	-25.6	0.4	1.5
	2	-25.5	0.4	1.4	-25.7	0.4	1.5
	3	-24.9	0.2	0.9	-24.9	0.4	1.6

5

6

1 Table 3. Calculations of the isotopic composition of CO₂ of the soil efflux using the chamber
 2 inlet and outlet data separately. Regressions with the chamber inlet data highlight the δ¹³C of
 3 soil efflux from the forest in general, and those with the chamber outlet data highlight the
 4 δ¹³C of soil efflux within the chambers. Two variations of mixing relationship were
 5 examined, following Keeling (1958) and Miller and Tans (2003), either with all chamber data
 6 or subsets for each chamber. Analysis of covariance was performed on the pair highlighted in
 7 bold and the intercepts were statistically different (ANCOVA, p < 0.0001). The standard
 8 errors of each slope or intercept are shown in parentheses. For the “difference” rows, the
 9 uncertainty in differences between pairs are shown in parentheses; n = number of samples.

10

		All chambers		Chamber 1		Chamber 2		Chamber 3	
		inlet	outlet	inlet	outlet	inlet	outlet	inlet	outlet
n		1284	1284	429	429	463	463	392	392
Keeling	slope	6997.3 (29.5)	6749.9 (39.3)	6951.4 (50.7)	6766.7 (58.0)	7014 (50.4)	7017.7 (65.7)	7025.7 (52.4)	6901.2 (78.7)
	intercept	-26.11 (0.07)	-25.53 (0.08)	-26.00 (0.12)	-25.61 (0.12)	-26.17 (0.12)	-26.10 (0.13)	-26.18 (0.12)	-25.73 (0.15)
	difference		0.58 (0.15)		0.39 (0.24)		0.07 (0.25)		0.45 (0.27)
	intercept	6989.9 (28.3)	6738.9 (39.3)	6939.8 (48.4)	6729.2 (57.1)	7002.8 (48.8)	6994.1 (65.6)	7029.3 (49.5)	6911.9 (79.3)
Miller- Tans	slope	-26.10 (0.07)	-25.51 (0.08)	-25.98 (0.11)	-25.53 (0.11)	-26.13 (0.11)	-26.06 (0.13)	-26.19 (0.12)	-25.75 (0.15)
	difference		0.59 (0.15)		0.45 (0.22)		0.07 (0.24)		0.44 (0.27)

11

12

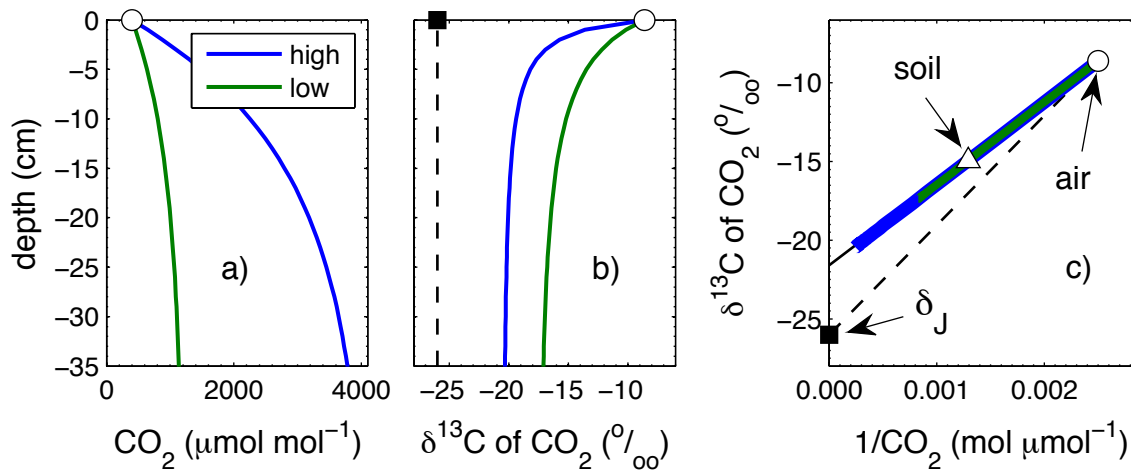
13

14

1 Table 4. Statistics for $\delta^{13}\text{C}$ of soil surface flux (δ_{R} , ‰) and $\delta^{13}\text{C}$ of production (δ_{J} , ‰) over the
 2 full two-month measurement period, and for the dry and moist periods. Data from all
 3 chambers were combined. SD = standard deviation, n=number of measurements. Overall
 4 frequency distributions and statistics for two-month period are shown in Fig. 8. Letters
 5 indicate means that were significantly different ($p < 0.0001$, Tukey's honest significant
 6 difference test).

	Depth	All data			Dry period			Moist period		
		Mean	SD	n	Mean	SD	n	Mean	SD	n
$\delta^{13}\text{C}$ of soil										
surface flux	surface	-25.6 ^d	1.1	1284	-25.4 ^c	1.1	117	-25.4 ^c	1.3	112
(δ_{R} , ‰)										
	O/A	-27.2 ^a	0.6	1050	-27.5 ^a	0.8	114	-27.2 ^a	0.5	112
$\delta^{13}\text{C}$ of	interface									
production	-5 cm	-26.2 ^b	0.3	1021	-26.2 ^b	0.4	110	-26.2 ^b	0.2	100
(δ_{J} , ‰)	-10 cm	-26.0 ^c	0.3	1153	-26.0 ^b	0.4	113	-26.0 ^b	0.4	104
	-30 cm	-26.0 ^c	0.3	1022	-26.0 ^b	0.3	111	-26.0 ^b	0.3	107

7



1

2 Figure 1. Modeled steady-state diffusive vertical profiles of a) soil pore space CO₂, b) δ¹³C of

3 soil pore space CO₂, and c) the relationship between them, shown for low and high flux rates

4 (colors). The CO₂ and δ¹³C of CO₂ in forest air at the soil-air boundary (C_a, δ_a) are shown

5 (circle) along with the δ¹³C of the CO₂ produced by respiration (δ_J, square and vertical dashed

6 line in b). The colored lines in a) and b) both plot on the upper (diffusive) solid line in c).

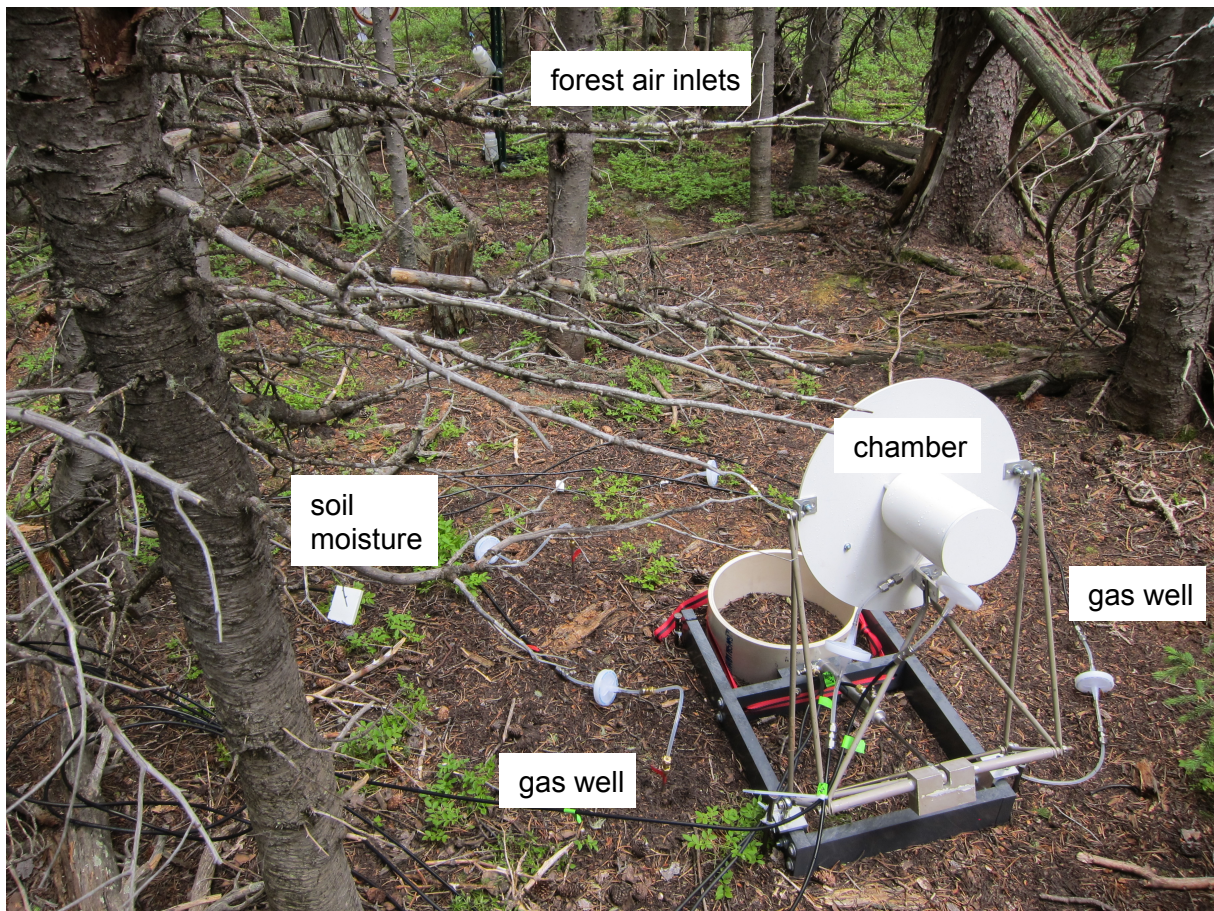
7 The triangle in c) denotes an individual gas well measurement of soil pore space (C_s, δ_s),

8 which when combined with measurements of forest air allows calculation of δ_J via Eq. 1.

9 Symbols are labeled in panel c) and are the same in all panels.

10

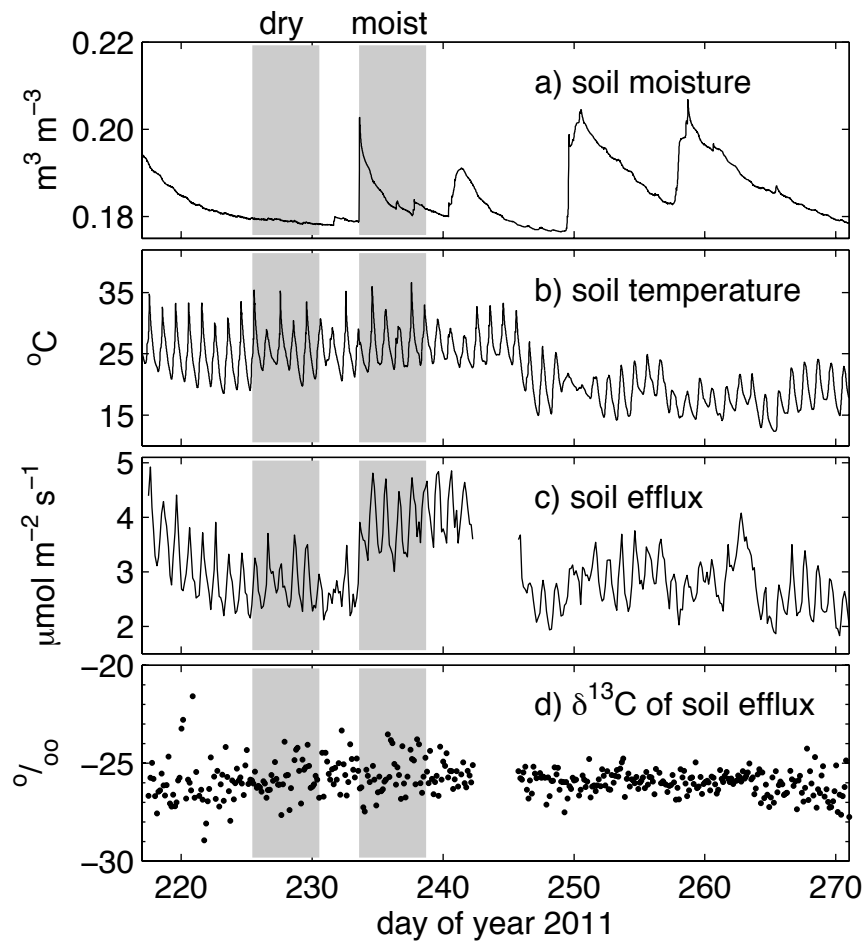
11



1

2 Figure 2. Instrumentation installed at the Niwot Ridge forest for this study, including an
3 automated soil surface flux chamber, the gas wells surrounding it (steel tubing inserted
4 vertically into the ground with white filters connected to black tubing), and the top of a soil
5 moisture probe. Inlets for forest air measurement can be seen at top, attached to a fencepost.

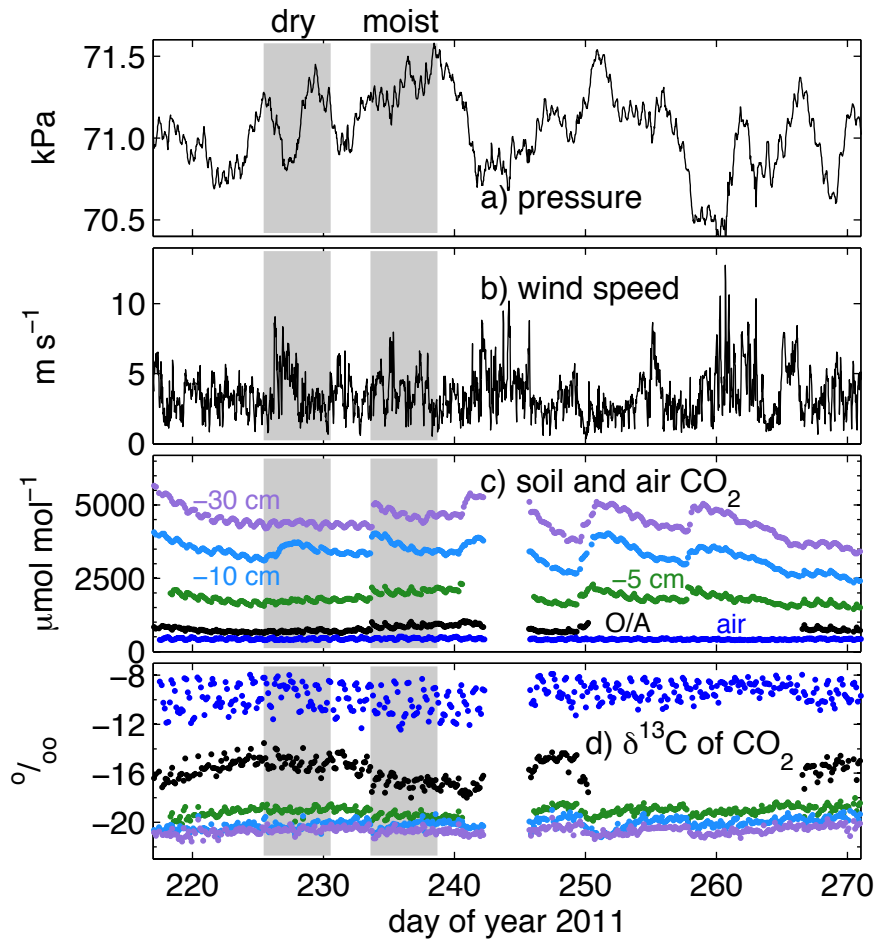
6



1

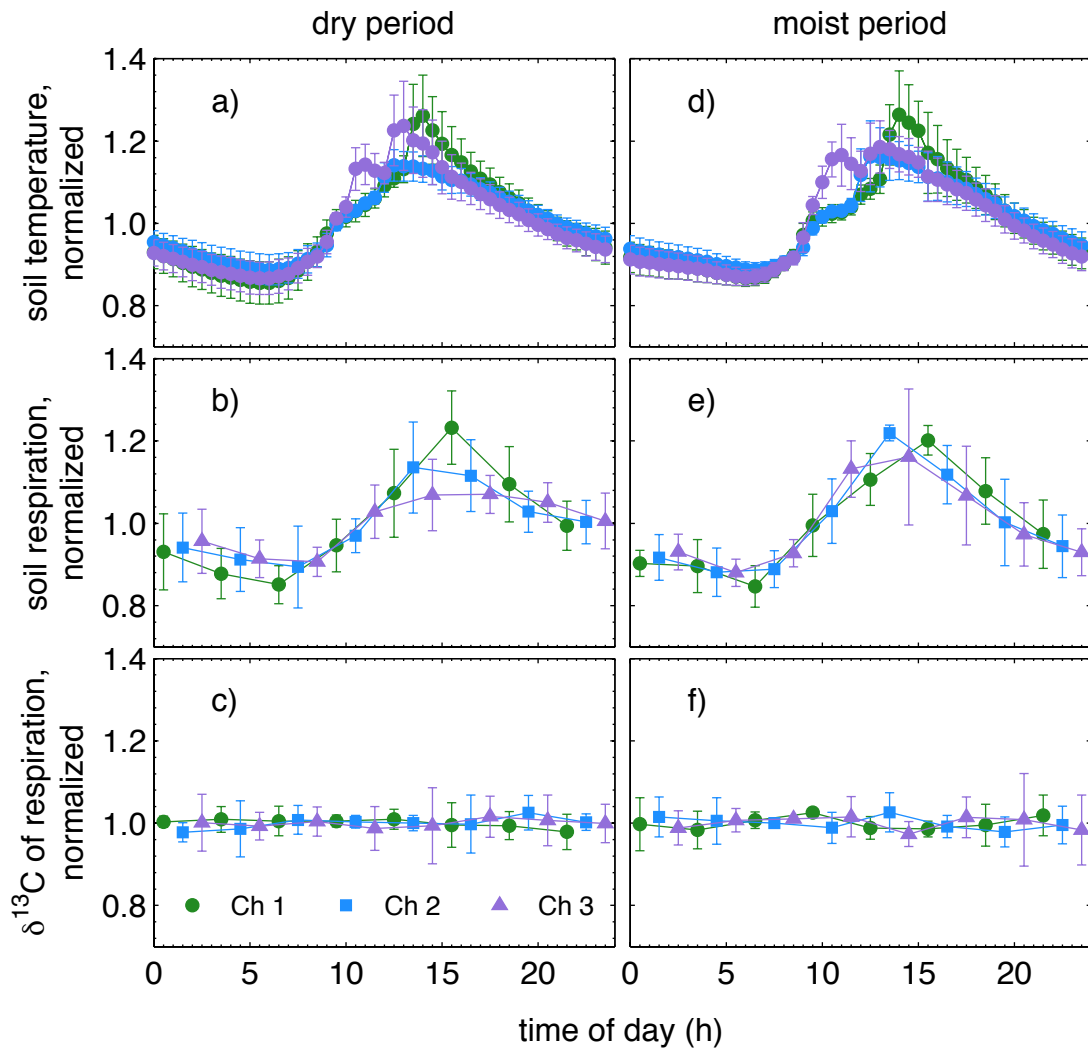
2 Figure 3. Soil moisture (0-10 cm), soil temperature (5 cm), soil efflux, and $\delta^{13}\text{C}$ of soil efflux
 3 (δ_{R}) measured at the location of chamber 1 over the duration of the experiment. Five-day dry
 4 and moist time periods are highlighted with shading.

5



1
2
3
4
5
6

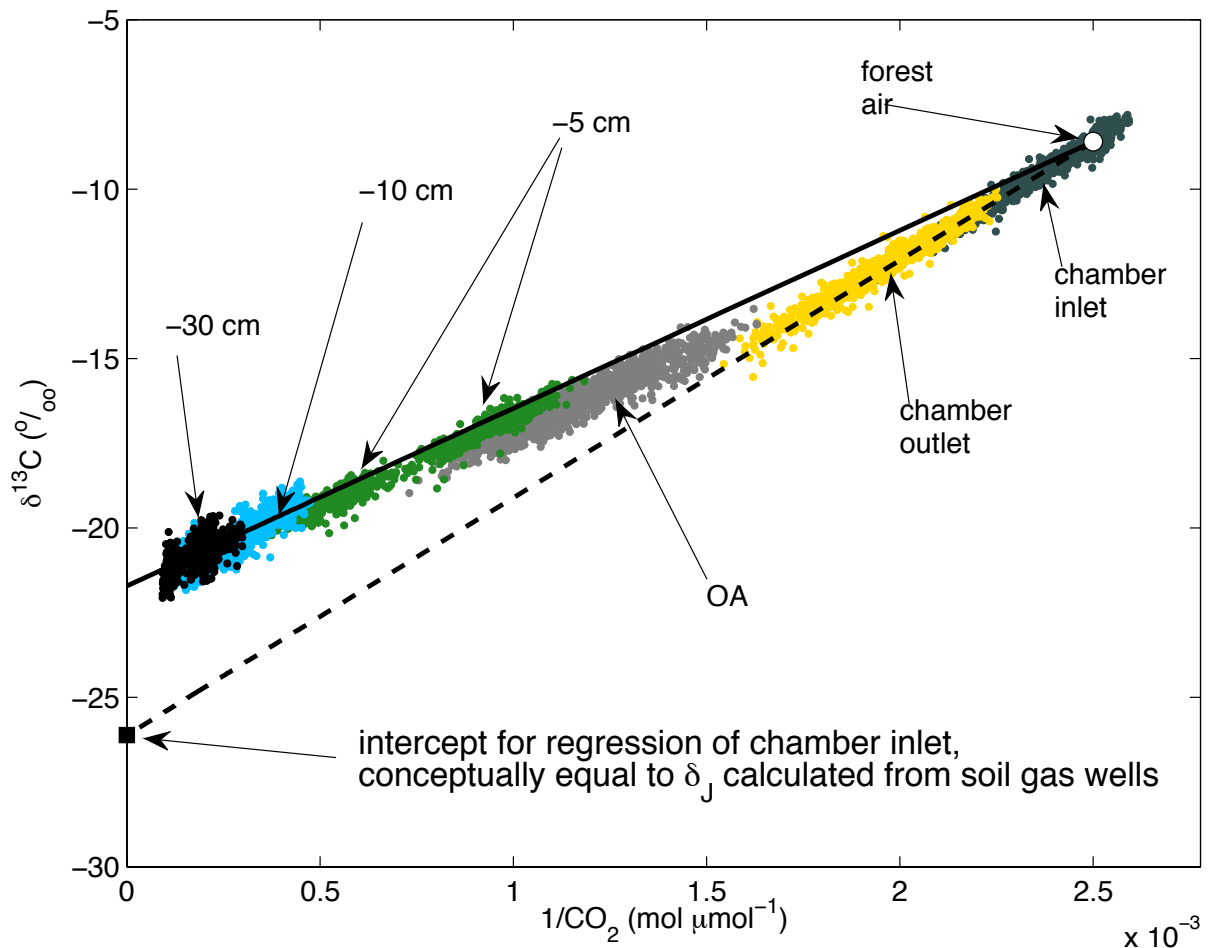
Figure 4. Barometric pressure (12 m), wind speed (21 m), CO₂ and δ¹³C of CO₂ in soil pore space and forest air measured at the location of chamber 1 over the duration of the experiment, with dry and moist time periods shaded. Depths of soil gas for c) and d) were at the O/A horizon interface, -5 cm, -10 cm, and -30 cm (colors indicated in c).



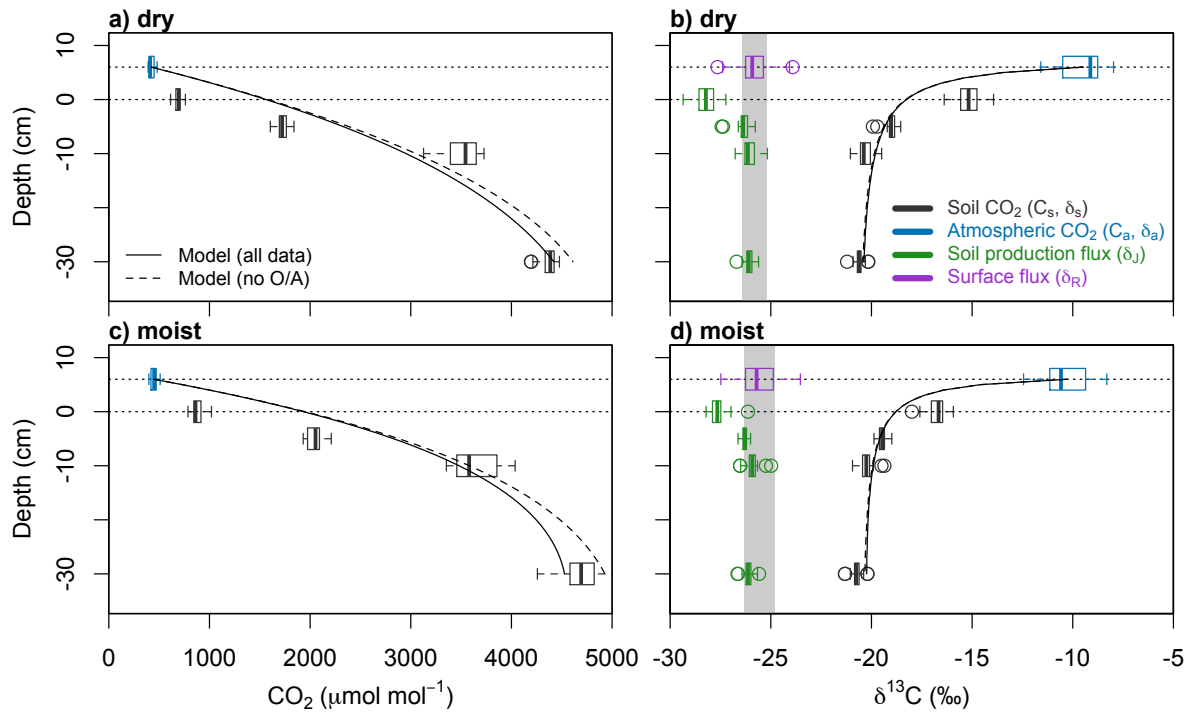
1

2 Figure 5. Mean (5-day) diel patterns of soil temperature (5 cm), soil surface flux, and $\delta^{13}\text{C}$ of
 3 soil surface flux (δ_R) during the dry (left) and moist (right) periods. Each time series was
 4 normalized by dividing by its 5-day mean. Data are shown for chambers 1, 2, and 3
 5 separately (legend in c). A non-normalized version of this plot can be found in Appendix A.

6



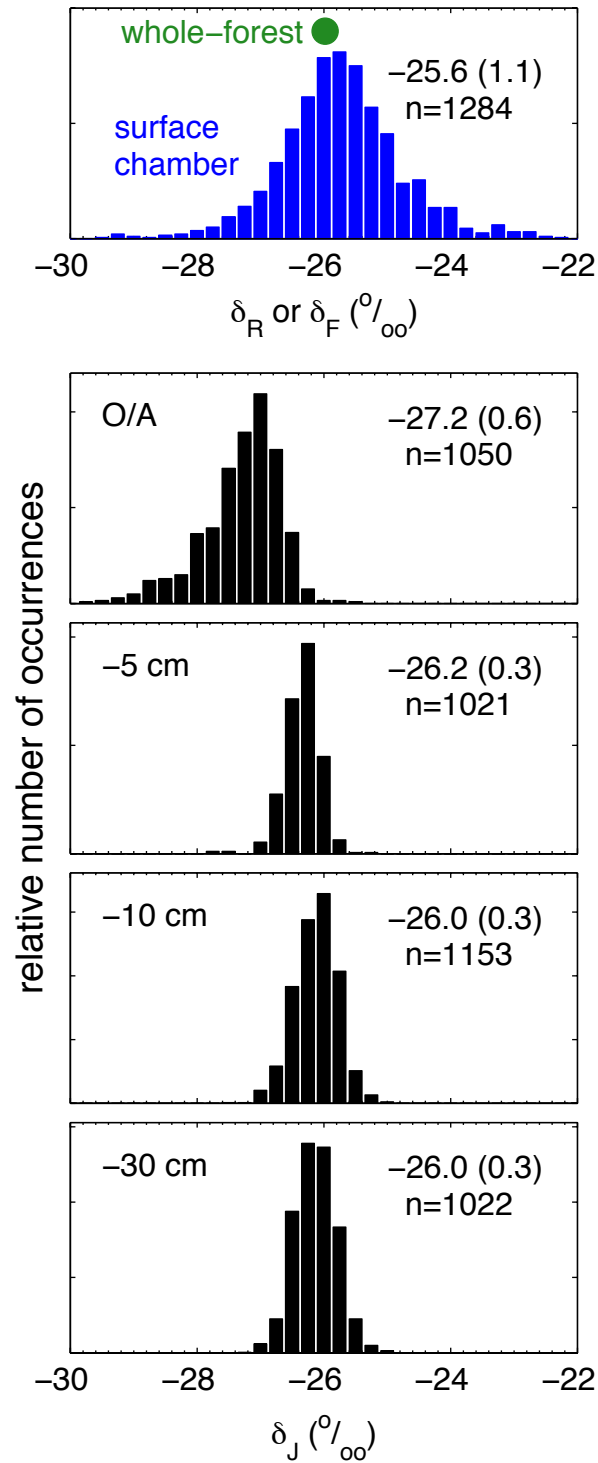
1
 2 Figure 6. Relationships between $\delta^{13}\text{C}$ and $1/\text{CO}_2$ measured at the chamber inlet and outlet,
 3 and in the soil pore space at 4 depths; all data from all locations are shown for the two-month
 4 experiment. The dashed line is a regression of the chamber inlet data ($\delta^{13}\text{C} = 6997/\text{CO}_2 - 26.1$
 5 ‰ , $n = 1284$, standard error of intercept = 0.07‰). The solid line represents the expected
 6 diffusive mixing relationship, and was drawn between the y-intercept (shifted 4.4‰ above
 7 the regression intercept) and an arbitrary indicator of forest air (white circle, -8.6‰ and
 8 $1/(400 \mu\text{mol mol}^{-1})$). Note the chamber inlet data are actual measurements of forest air, and
 9 illustrate its variability. Note also that the data from the O/A interface and 5 cm depth fall
 10 between these lines due to the experimental artifact described in the text.
 11



1

2 Figure 7. Measured profiles of soil pore space and atmospheric CO₂, δ¹³C of soil pore space
 3 and atmospheric CO₂, for the 5-day dry and moist periods for chamber 1 (other chambers
 4 were similar). Atmospheric measurements (blue) were made at the inlet of the automated
 5 chamber. These are compared to the δ¹³C of soil surface flux (δ_R, purple) measured by the
 6 automated chamber, and to the δ¹³C of the CO₂ produced by respiration (δ_J, green, calculated
 7 from the measurements in black and blue using Eq. 1). Box and whisker diagrams are used to
 8 indicate statistical distributions using the median (central line) and 25th and 75th percentiles
 9 (box edges). Data exceeding the interquartile range by a factor of 1.5 are denoted as outliers
 10 (circles). The gray rectangles in the right panels are shown at the 25th and 75th percentiles for
 11 δ_R (purple), to facilitate comparison with δ_J (green). Lines show the results of the best-fit
 12 diffusion model (see text) compared to either all measurement depths (solid line) or (dashed)
 13 excluding the O/A interface (0 cm). Horizontal dotted lines at 0 cm and 6 cm indicate the
 14 O/A interface and the top of the O horizon, respectively.

15



1

2 Figure 8. Frequency distributions of all measurements at all locations over the two-month
 3 duration of the experiment, of $\delta^{13}\text{C}$ of soil surface flux (δ_R) measured by automated chambers,
 4 and $\delta^{13}\text{C}$ of the CO_2 produced by respiration (δ_J) at each depth. Numbers on the plots are
 5 means, standard deviations, and sample size. Also shown on the top panel (circle) is the mean
 6 for the $\delta^{13}\text{C}$ of whole-forest respiration (δ_F) determined from measurements of forest air for

1 this time period reported by Bowling et al. (2014) (the uncertainty is smaller than the
2 symbol). Deviations in the mean of δ_j at the O/A interface from δ_R were caused by
3 experimentally-induced advection as discussed in the text.

4